ESD-TDR-64-135

TM-03973

A RE-ENTRY VEHICLE SIMULATION DESIGNED FOR THE STUDY OF GROUND SYSTEM REQUIREMENTS

TECHNICAL DOCUMENTARY REPORT NO.   ESD-TDR-64-135

JULY 1964

P. J. Plender

Prepared for

DEPUTY FOR ADVANCED PLANNING

ELECTRONIC SYSTEMS DIVISION

AIR FORCE SYSTEMS COMMAND

UNITED STATES AIR FORCE

L. G. Hanscom Field, Bedford, Massachusetts

Project No. 611.1

Prepared by

THE MITRE CORPORATION
Bedford, Massachusetts
Contract AF19(628)-2390

AD060374

A RE-ENTRY VEHICLE SIMULATION DESIGNED FOR THE STUDY OF

GROUND SYSTEM REQUIREMENTS

TECHNICAL DOCUMENTARY REPORT NO.   ESD-TDR-64-135

JULY 1964

P. J. Plender

Prepared for

DEPUTY FOR ADVANCED PLANNING

ELECTRONIC SYSTEMS DIVISION

AIR FORCE SYSTEMS COMMAND

UNITED STATES AIR FORCE

L. G. Hanscom Field, Bedford, Massachusetts

Project No. 611. 1

Prepared by

THE MITRE CORPORATION
Bedford, Massachusetts
Contract AF19(628)-2390

FOREWORD

The valuable work of programming the equations for
machine solution was performed by members of The
MITRE Corporation's Computer Applications Department.
The analog program was produced by M. Santarelli, and
the digital program was developed by K. Erat, P. Moskovites
and J. Whipple.

ABSTRACT

A computer simulation of re-entry vehicle trajectories
has been developed as an aid in determining the require-
ments of supporting ground-based electronic systems.
This report describes the mathematical model used in the
simulation and discusses, with the aid of examples, the
usefulness of the output data in the preliminary design
of tracking and communications networks.

REVIEW AND APPROVAL

This technical documentary report has been reviewed and
is approved.

VERNON A. DANDER
Capt., USAF
Project Officer

TABLE OF CONTENTS

ILLUSTRATIONS

vii

1. INTRODUCTION

The entry of ballistic and space vehicles into the earth's atmosphere has long been of interest to the Air Force. Earlier, interest centered on the problems associated with ballistic missile re-entry vehicles. Today, this interest has been broadened to include manned ballistic vehicles, like the Gemini and Apollo capsules, and maneuverable lifting vehicles of the X-20 type. Accompanying the development of these diverse vehicles, there has of course been an impressive growth of ground-based electronic systems supporting vehicle testing and operation. As the Air Force's role in space operations develops, a continuing need can be expected for quantitative data on which to base the design of these electronic systems.

This memorandum describes a computer simulation of re-entry which has been developed as a means of generating some of the quantitative information needed in ground system design. The complete simulation is programmed to run on the IBM 7030 digital computer, but an abridged version has also been developed for use on MITRE's PACE analog computer. The mathematical model which forms the basis of the computer program is discussed, and typical results produced by the two computers are presented.

Section 2, which follows, discusses some specific questions concerning ground system design for which the simulation can provide useful answers. In Sections 3 through 9, the organization and content of the simulation are described and important assumptions are given. Some actual results of operating the simulated system on both analog and digital computers are presented in Section 10.

2. USE OF VEHICLE SIMULATION IN COMMAND AND CONTROL STUDIES

The actions of a ground-based electronic system supporting the mission of an aerospace vehicle are intimately related to the motion and activities of the vehicle itself. Analysis of the vehicle's mission and

1

performance is therefore a prerequisite for determining the functional and technical requirements of such a ground system. Simulation provides the means for this analysis and permits interactions between the vehicle and the ground system to be observed while these individual systems are still in the planning stage. Simulation furnishes the quantitative information necessary for specifying quantitative ground system requirements. In the case of the present simulation, the data generated and the questions these data can help to answer are as follows. (All data are produced as functions of time.)

2.1 Line-of-Sight Range from Each Tracking Site to the Re-Entry Vehicle

A time history of range between the vehicle and ground stations is a necessity in the rational solution of range-dependent tracking and communication problems. Path loss, a basic variable in radar tracking and communication, is an explicit function of line-of-sight range. Whether the immediate design problem concerns required transmitter power, communication bandwidth, or the contribution of receiver thermal noise to radar tracking error, range is a variable which must be known.

2.2 Line-of-Sight Range Rate

Knowledge of the range rate expected at a given ground station during the tracking period is useful for two reasons. First, it permits the calculation of Doppler shift in signals sent between the vehicle and the ground. Secondly, with a knowledge of a given radar's range tracker characteristics, it enables one to estimate the range tracking errors that would be produced in that radar, as a function of time.

2.3 Elevation Angle of Line of Sight between Each Tracking Site and the Vehicle

By observing the time history of elevation angle at each tracking site, it is a simple matter to determine when the vehicle is above the radar horizon at that station and thus find out when that station can track and communicate with the vehicle, given that the range between the two is not restrictive. With this basic information for all ground stations, and with a knowledge of the communications

2

traffic through each station when it is actively tracking, a time history of total traffic throughout the ground communications network can be constructed. This information will give directly the traffic handling requirements of the various segments of the ground network.

The history of vehicle visibility from the tracking stations can be used in conjunction with the corresponding range histories to evaluate the effectiveness of various deployments of ground stations. In comparing various deployments of a fixed number of stations, the criterion of effectiveness might be the total length of time during which the vehicle is simultaneously visible (at positive elevation angle) and within a specified range of one or more stations. Alternatively, the problem might be to choose a re-entry trajectory which would make maximum use of an existing ground system configuration.

2.4 Effect of Ground Control Delays and Errors on Vehicle Trajectory

The response of maneuverable re-entry vehicles to guidance and control actions is manifested in the character of the trajectory, in the time histories of vehicle accelerations and skin temperatures, and in the location of the terminal point relative to the intended destination. The effects of errors and time delays in vehicle guidance commands can be determined, therefore, by observing these same quantities. Ascertaining these effects is vital in any study aimed at determining the feasibility of emergency guidance of maneuverable vehicles by the ground system.

3. COORDINATE SYSTEMS

It will be useful to define at the outset the coordinate systems in which vehicle position, velocity, and body attitude are measured.

3.1 Position Coordinates

Vehicle position is measured with respect to a rotating, spherical earth. The three position coordinates, shown in Fig. 1, are longitude θ, latitude φ, and radius r from the center of the earth.

3
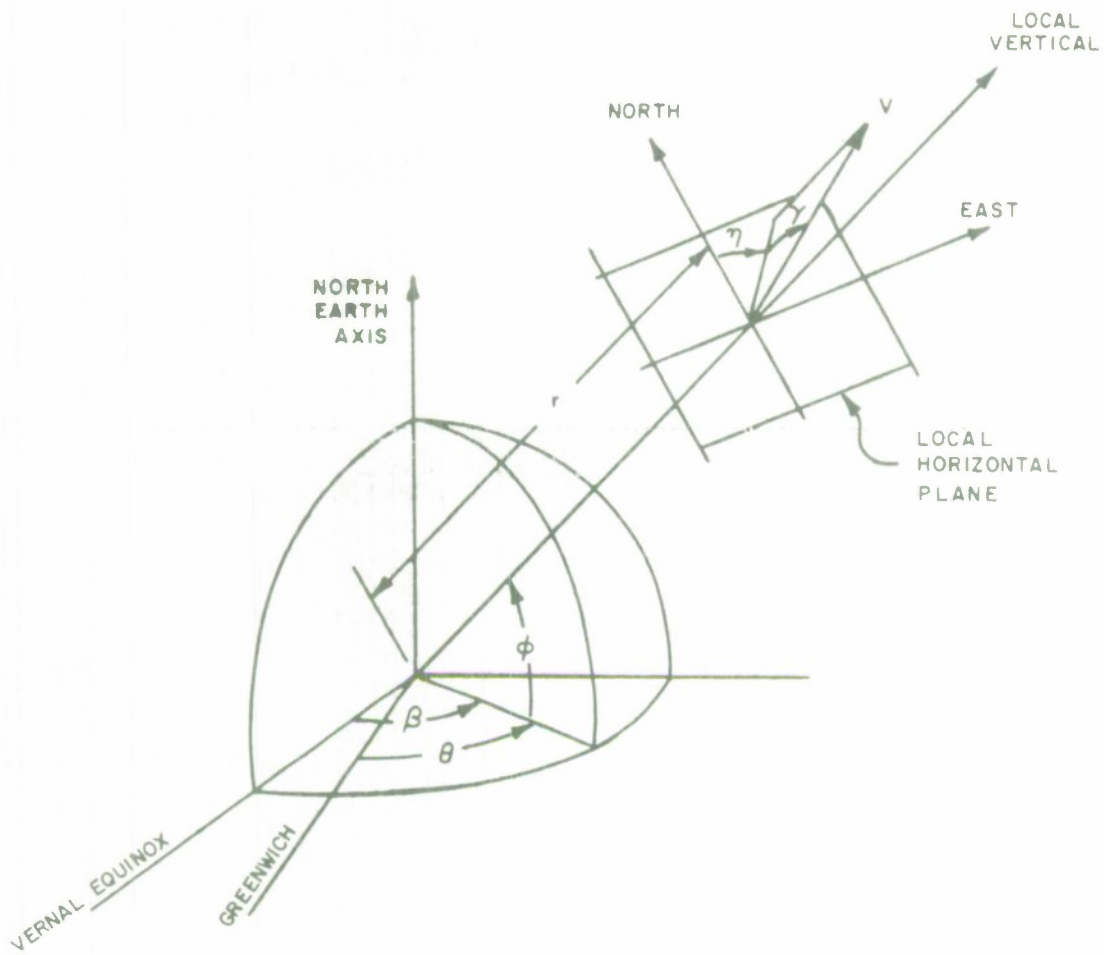
POSITION AND VELOCITY COORDINATE SYSTEMS

FIG. 1

A secondary set of coordinates, the downrange and cross-range distances of the projected position on the earth's surface from the initial position, is illustrated in Fig. 2. The downrange axis is a great circle, the plane of which contains the vehicle's initial velocity vector. The crossrange axis is the varying great circle which passes through the instantaneous projected position and intersects the downrange axis at right angles. Referring to Fig. 2, downrange and crossrange distances are defined as the length of the arc $\underline{a}$ along the downrange axis and the length of the arc $\underline{b}$ along the crossrange axis, respectively.

3.2 Velocity Coordinates

Considered as a point mass, the vehicle has a velocity of magnitude V relative to earth axes, in a direction defined by the angles η and γ, as shown in Fig. 1. The angle η represents the vehicle's heading with respect to north; the angle γ is the angle of the velocity vector above the local horizontal plane.

3.3 Body Attitude Coordinates

The vehicle is assumed to maneuver with zero sideslip at all times. Body attitude is then defined by angle of attack α and bank angle σ, as depicted in Fig. 3. Angle of attack, of course, is the angle between the vehicle's longitudinal reference axis and the velocity vector. The bank angle is the angle between the lift vector and the vertical plane containing the velocity vector.

4. ORGANIZATION OF COMPUTER PROGRAMS

A re-entry vehicle may be any of a number of types. In its simplest form, it is an uncontrolled body, falling ballistically through the atmosphere. In a more sophisticated form, it may contain a closed-loop guidance and control system which, by modulating the aerodynamic forces on the vehicle, brings it to some specified terminal conditions of position and velocity. The Mercury capsule is an example of the first type, whereas the latter type is represented by the X-20.

NORTH
AXIS

EARTH'S SURFACE

PROJECTION OF
PRESENT POSITION

a

b

ψ η_o

c

PROJECTION OF
ORIGINAL POSITION

(ϕ_o, θ_o)

(ϕ, θ)

EQUATORIAL
PLANE

$R_e a$ = DOWNRANGE DISTANCE

$R_e b$ = CROSSRANGE DISTANCE
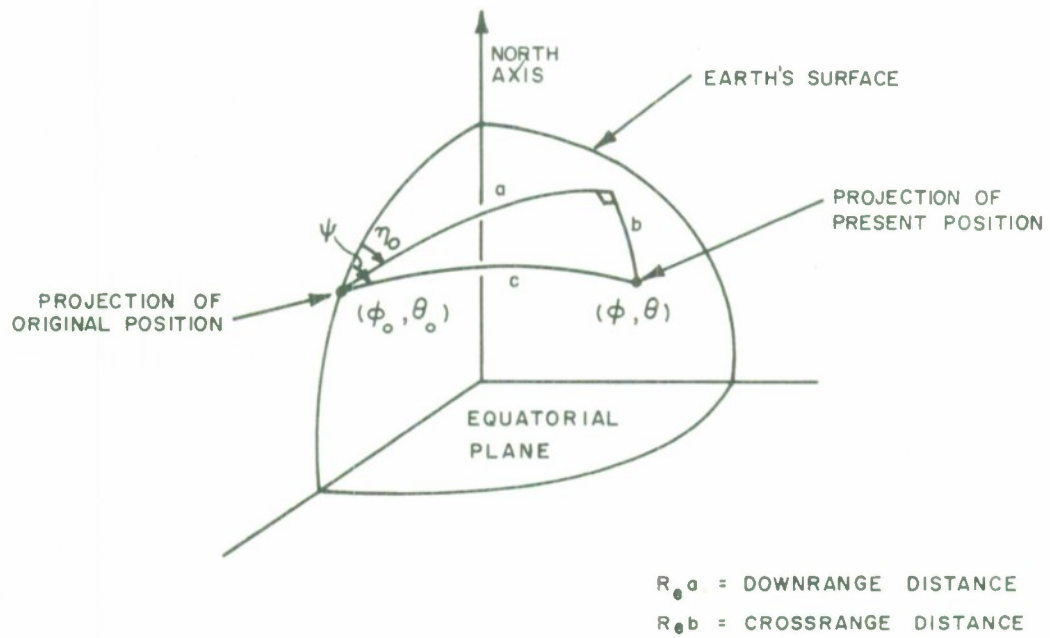
DOWNRANGE AND CROSSRANGE POSITION COORDINATES

FIG. 2
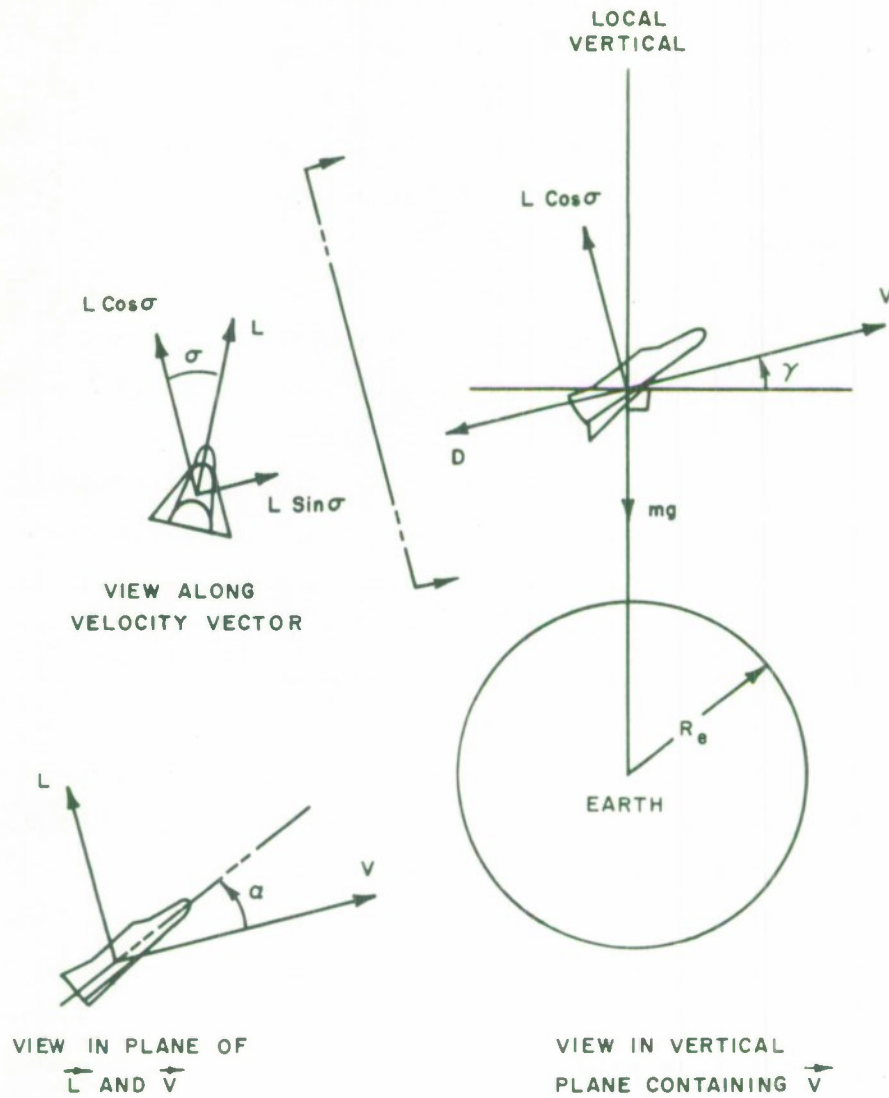
FORCE SYSTEM AND VEHICLE BODY ATTITUDE

FIG. 3

To make the computer programs applicable to the widest range of re-entry vehicle types and to simplify later expansion in the scope of the simulations, the programs were constructed in modular form. In the case of the digital program, this means that nearly all computations are done in subprograms, and the main program is in effect an executive program. Changes in the system being simulated are easily made by changing appropriate subprograms.

Figure 4 is a block diagram showing the over-all organization of the simulation. The most basic part is that identified as "Vehicle Dynamics"--the subprogram relating position and velocity of the vehicle to bank angle and aerodynamic lift and drag coefficients. Position and velocity are derived in this section of the simulation by machine integration of the differential equations of motion. Guidance computations, based primarily on instantaneous position and velocity, are performed in an independent subprogram. The guidance system determines the desired instantaneous bank angle and lift-to-drag ratio. In the Aerodynamic Data subprogram, lift-to-drag ratio is translated into angle of attack, lift coefficient, and drag coefficient, by means of tabulated aerodynamic characteristics of the vehicle. Local atmospheric density, required in many computations, is computed from vehicle altitude in the subprogram called "Model Atmosphere". Operating together, these four subprograms produce a time history of the vehicle's position, velocity, and attitude.

Three other subprograms draw upon these results and periodically compute the following information:

(a) Downrange and crossrange components of the vehicle's position.

(b) Specific force per unit mass on the vehicle (or "acceleration" felt by the crew in a manned vehicle).

(c) Critical structural temperatures.

(d) Antenna gimbal angles and geometric range and range rate of ground based stations tracking the vehicle.

8
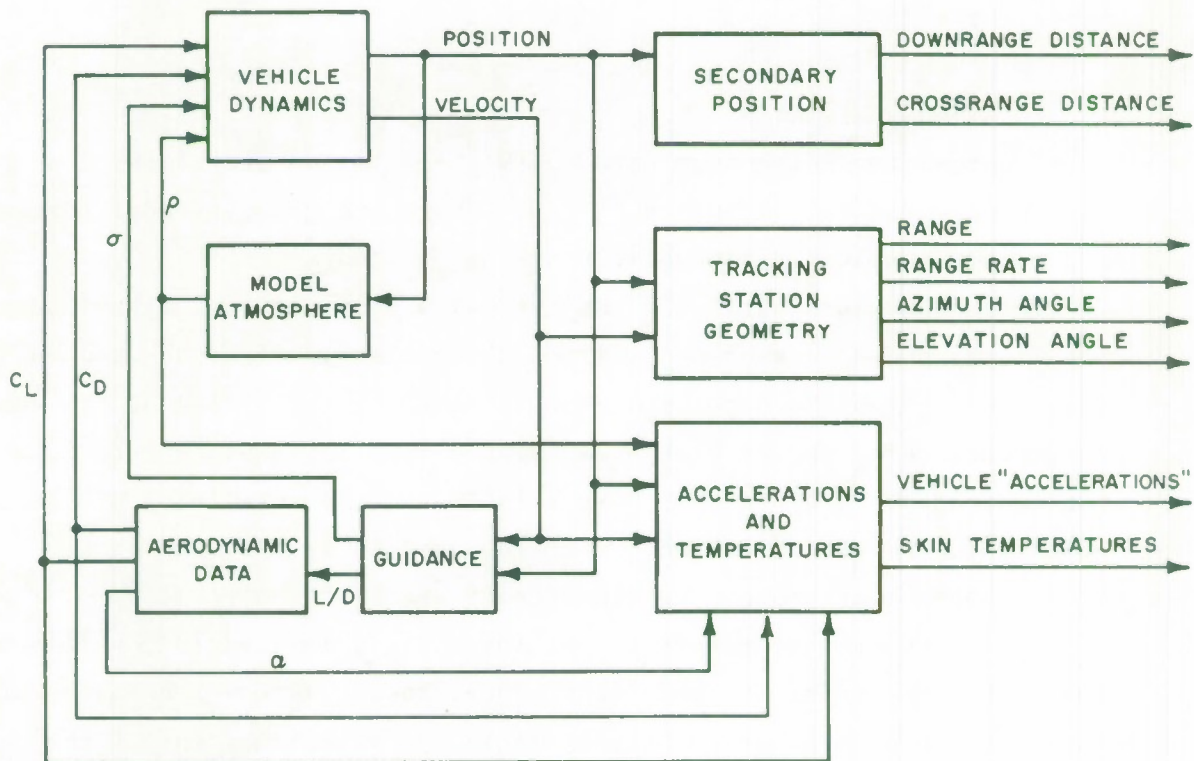
BLOCK DIAGRAM OF SIMULATION

FIG. 4

The digital computer program encompasses all the parts just des-
cribed. Due to equipment limitations, however, the analog simulation
does not include tracking station geometry and does not compute position
in terms of downrange and crossrange distances. For the same reason,
the guidance system in the analog simulation is restricted to relatively
simple types.

5. EQUATIONS OF MOTION

The equations of motion used in this simulation are those of a
point mass under the influence of lift, drag, and gravitational forces.
Rotational dynamics of the vehicle are not included.

The assumption justifying the exclusion of rotational dynamics is
that if the guidance system calls for a given angle of attack and bank
angle, the attitude control system or flight control system of the vehicle
can produce those angles with a negligible time lag. Since rotational
time constants are extremely short relative to the total time of flight,
and only the resultant trajectory of the vehicle is of interest here,
this assumption introduces no significant error in the results.

An inverse-square gravitational force field is used in the simula-
tion. To first-order accuracy, therefore, the equations are valid for
unpowered vehicles at any altitude, including satellites out of the
sensible atmosphere, vehicles within the atmosphere, and re-entry vehicles
passing from free space through the atmosphere to the surface of the
earth.

The equations of motion and their derivation are given in
Appendix A.

6. GUIDANCE SYSTEM

Whereas the equations of motion are the same for any vehicle,
there is virtually no limit to the number of guidance laws which may
control a re-entry vehicle's trajectory. For the case of lifting re-
entry vehicles, the manifold possibilities in guidance system design

10

are enumerated and discussed in broad perspective in Ref. 1. As the 98-reference bibliography of Ref. 1 attests, there is a large body of literature on the subject of re-entry guidance.

The computer programs are so organized that a wide variety of guidance techniques can be simulated. By proper choice of guidance equations and aerodynamic data, both unguided ballistic re-entry bodies and maneuverable re-entry gliders with relatively complex guidance systems can be accommodated.

The guidance systems used in producing the results reported in this memorandum are discussed in Appendix C. The analog simulation used a constant bank angle and a lift-to-drag ratio which was varied about a fixed nominal value by an altitude - rate damping law. The digital simulation contained a more complex scheme. Guidance commands were based on both altitude rate and the position of the desired destination with respect to the locus of attainable destinations, the latter being calculated from approximate, closed-form equations. This prediction - type guidance scheme is similar to those described in Refs. 2, 3, and 4. The closed-form prediction equations are developed in Appendix B.

It has often been suggested that a ground-based guidance capability be provided for maneuverable re-entry vehicles, as a means of controlling the trajectories of vehicles which have suffered primary guidance system failures. Such a back-up guidance system would make radar measurements of the vehicle's trajectory, collect telemetered data on various flight variables, and compute guidance commands on the ground. The commands would be transmitted to the vehicle through a ground-to-vehicle data link. Many problems can be visualized in this mode of guidance; one of these is the possible adverse effect of data processing delays on the vehicle trajectory. To permit investigation of this problem, the digital simulation incorporates the option of introducing a time delay of as much as 60 seconds between calculation of the guidance commands and application of these commands to the vehicle's flight control system.

11

7. ACCELERATIONS AND STRUCTURAL TEMPERATURES

Accelerations felt by human crew members and temperatures of critical parts of the vehicle skin must be kept under certain limits during re-entry. It is therefore necessary to know the history of these variables throughout a simulated flight. With nomenclature as defined in the list of symbols, components of specific force per unit mass along the vehicle's body axes are as follows:

Longitudinally (positive aft):

$$m_L = \frac{qA}{mg_e} \left[C_D \text{ Cos } \alpha - C_L \text{ Sin } \alpha \right] \tag{1}$$

Laterally, in the plane formed by the longitudinal axis and the lift vector (positive upward):

$$n_n = \frac{qA}{mg_e} \left[C_D \text{ Sin } \alpha + C_L \text{ Cos } \alpha \right] \tag{2}$$

The resultant value is

$$n = \frac{qA}{mg_e} \sqrt{C_D^2 + C_L^2} \tag{3}$$

In this simulation, temperatures are computed at two critical points on the surface of a winged re-entry vehicle: the stagnation point and the bottom of the wing. The equations are based on the assumptions that these outer surfaces are radiation-cooled and that the flow over the surfaces is laminar. Stagnation-point temperature is given by the equation (Refs. 2 and 5).

$$T_S = \frac{13880.}{F_N^{1/8}} \left[\frac{\rho \left(\frac{\text{lb. sec.}^2}{\text{ft.}^4} \right)}{2.3769 \times 10^{-3}} \right]^{1/8} \left[\frac{V}{V_c} \right]^{0.788} \quad \text{degrees F. abs.} \tag{4}$$

where

$$F_N \equiv R_N \, \epsilon_N^{\ 2} \quad \text{feet.} \tag{5}$$

Wing-bottom temperature is as follows (Ref. 2):

$$T_{WB} = K_{WB} \, (qC_L)^{0.2} \, v^{0.467} \quad \text{degrees F. abs.} \tag{6}$$

8.   DOWNRANGE AND CROSSRANGE PROJECTIONS OF VEHICLE POSITION

Downrange and crossrange components of the vehicle's projected
position have been defined in Section 3.1 and in Fig. 2. Equations for
these position components can be derived from Figs. 1 and 2 by the
standard methods of spherical trigonometry. It is easily verified that
calculation of these distances requires the solution of the following
set of equations:

$$c = \mathrm{Cos}^{-1} \left[\mathrm{Sin}\, \varphi \, \mathrm{Sin}\, \varphi_o + \mathrm{Cos}\, \varphi \, \mathrm{Cos}\, \varphi_o \, \mathrm{Cos}\, (\theta - \theta_o) \right] \tag{7}$$

$$\Psi = \mathrm{Sin}^{-1} \left[\frac{\mathrm{Cos}\, \varphi \, \mathrm{Sin}\, (\theta - \theta_o)}{\mathrm{Sin}\, c} \right] \tag{8}$$

$$a = \mathrm{Tan}^{-1} \left[\frac{\mathrm{Cos}\, (\Psi - \eta_o)}{\mathrm{Cot}\, c} \right] \tag{9}$$

$$b = \mathrm{Sin}^{-1} \left[\mathrm{Sin}\, (\Psi - \eta_o) \, \mathrm{Sin}\, c \right] \tag{10}$$

$$\text{Downrange distance} = R_e a \tag{11}$$

$$\text{Crossrange distance} = R_e b \tag{12}$$

13

9. TRACKING STATION MEASUREMENTS

Ground-based tracking stations are represented in the digital simulation. For each of ten stations, the program computes the range, range rate, azimuth angle, and elevation angle that could be measured by a radar tracking the re-entry vehicle.

Figure 5 shows the re-entry vehicle's position relative to the coordinate system center at the ith tracking site. In terms of the local $x_i y_i z_i$ coordinate system, vehicle position is

$$x_i = r \, \text{Cos} \, \varphi \, \text{Sin} \, (\theta - \theta_i) \tag{13}$$

$$y_i = r \left[\text{Sin} \, \varphi \, \text{Cos} \, \varphi_i - \text{Cos} \, \varphi \, \text{Sin} \, \varphi_i \, \text{Cos} \, (\theta - \theta_i) \right] \tag{14}$$

$$z_i = r \left[\text{Sin} \, \varphi \, \text{Sin} \, \varphi_i + \text{Cos} \, \varphi \, \text{Cos} \, \varphi_i \, \text{Cos} \, (\theta - \theta_i) \right] - r_i \tag{15}$$

where

$$r_i = R_e + h_i \tag{16}$$

The slant range from the tracking station to the vehicle is

$$R_i = \sqrt{x_i^2 + y_i^2 + z_i^2} \tag{17}$$

Azimuth and elevation angles are given by the equations

$$A_i = \text{Tan}^{-1} \left[\frac{x_i}{y_i} \right] \tag{18}$$

$$E_i = \text{Sin}^{-1} \left[\frac{z_i}{R_i} \right] \tag{19}$$

LOCAL
VERTICAL
(Z_i)

VEHICLE

$i^{\underline{th}}$ TRACKING SITE
(COORDINATES θ_i, ϕ_i, h_i)

R_i

E_i

NORTH (Y_i)

A_i

EAST (X_i)
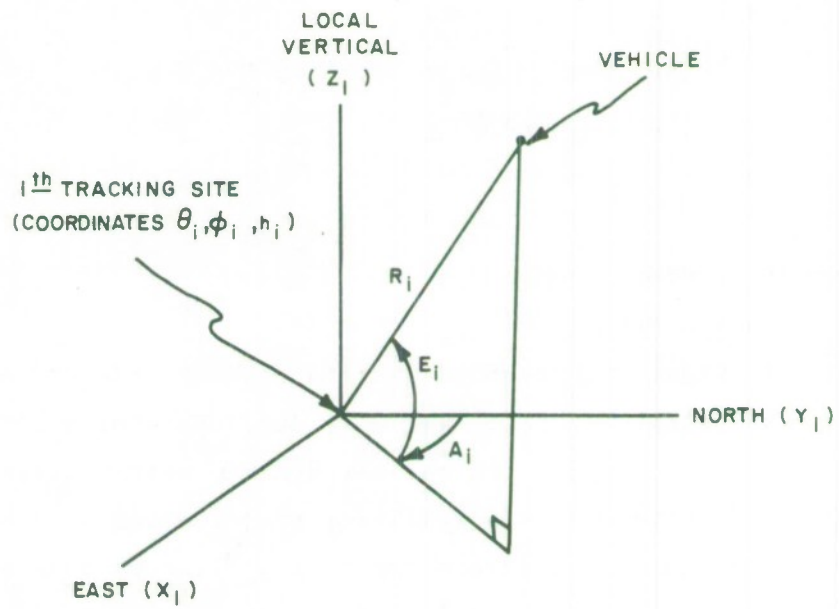
VEHICLE POSITION WITH RESPECT TO TRACKING SITE

FIG. 5

IA – 13 115

15

By differentiating the above equation for R_i and using Eqs. 13, 14, and 15 above and A-21, A-22, and A-23 of Appendix A to simplify the result, it can be verified that range rate is given by the expression

$$\dot{R}_i = V\left[\ \frac{r_i}{R_i}\ \right]\left\{ Sin\ \gamma\left[\frac{r}{r_i}\ -\ \frac{r_i + z_i}{r}\right]\right.$$

$$\left. -\ Cos\gamma\ \left[\ Cos\eta\ \left(Cos\varphi Sin\varphi_i - Sin\varphi Cos\varphi_i Cos(\theta-\theta_i)\right) - Sin\eta Cos\varphi_i Sin(\theta-\theta_i)\right]\right\}$$

$$(20)$$

10. RESULTS OF SIMULATIONS

10.1 Analog Results

In Figs. 8 through 13 there are shown some trajectories produced by the analog computer. All were developed for a lifting re-entry vehicle of the X-20 type, with the aerodynamic characteristics given in Figs. 6 and 7. Figure 8 is a family of trajectories at constant angle of attack (and constant lift-to-drag ratio, $\frac{L}{D}$), zero bank angle, and varying initial flight path angle. The characteristic lightly-damped phugoid oscillation is apparent, and the figure shows clearly the large effect that small variations in initial conditions can have on the motion of a vehicle of this type if re-entry is made at constant L/D.

In Fig. 9, altitude, velocity, dynamic pressure, stagnation-point skin temperature, and resultant specific force per unit mass during a near-equilibrium glide are presented as functions of time. In this case, the phugoid motion is damped by an altitude-rate feedback scheme which varies L/D around a nominal value of 1.5.

The practical effects of damping the natural trajectory oscillations is illustrated in Fig. 10. Altitude, stagnation-point skin temperature, and "acceleration" are presented as functions of time for two re-entry trajectories having identical initial conditions. In one trajectory, the re-entry vehicle maintains constant L/D, and the

16
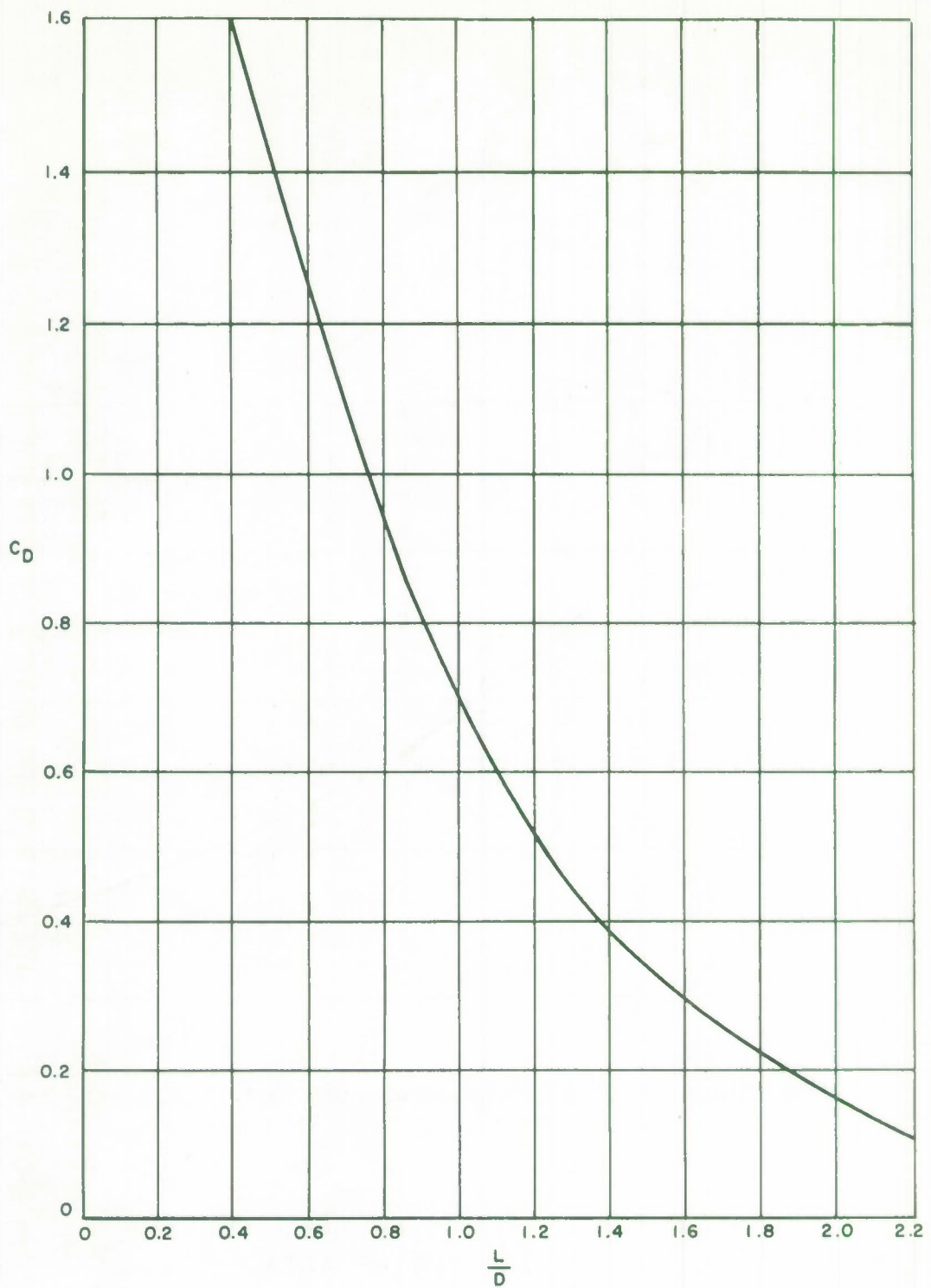
FIG. 6
DRAG COEFFICIENT VS. LIFT-TO-DRAG RATIO
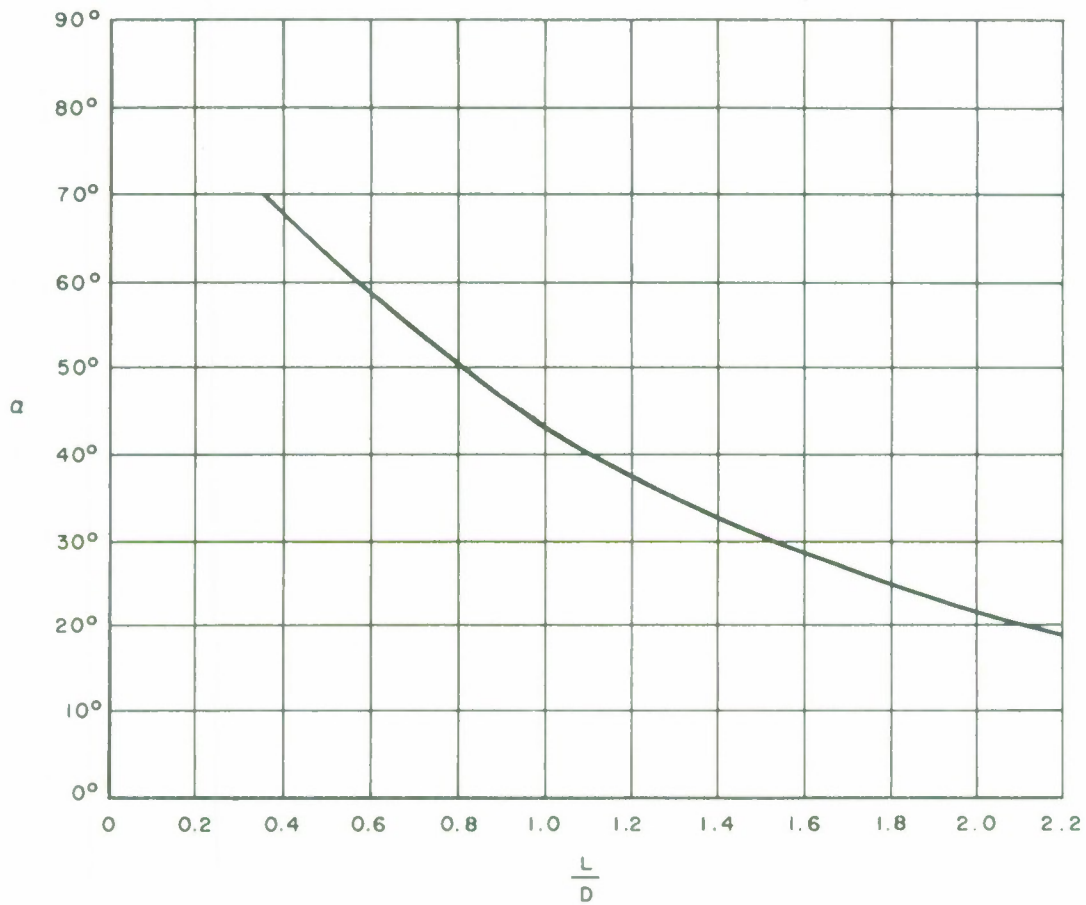
FIG. 7

ANGLE OF ATTACK
VS.
LIFT-TO-DRAG RATIO

18
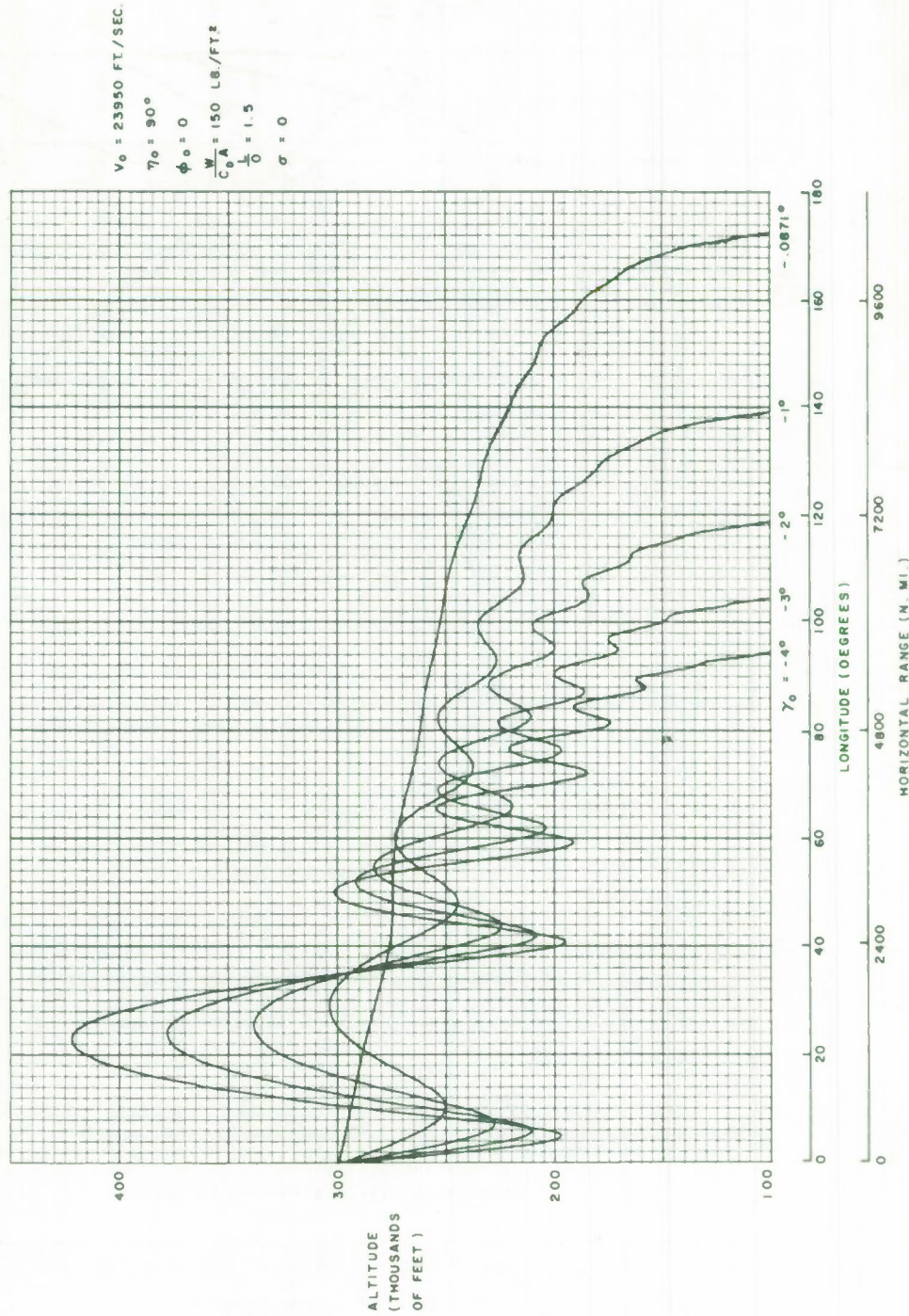
FIG 8
RE-ENTRY AT CONSTANT $\frac{L}{D}$

$V_0 = 23950$ FT/SEC.

$\eta_0 = 90°$

$\phi_0 = 0$

$\frac{W}{C_D A} = 150$ LB./FT.²

$\frac{L}{D} = 1.5$

$\sigma = 0$

IB-13 105
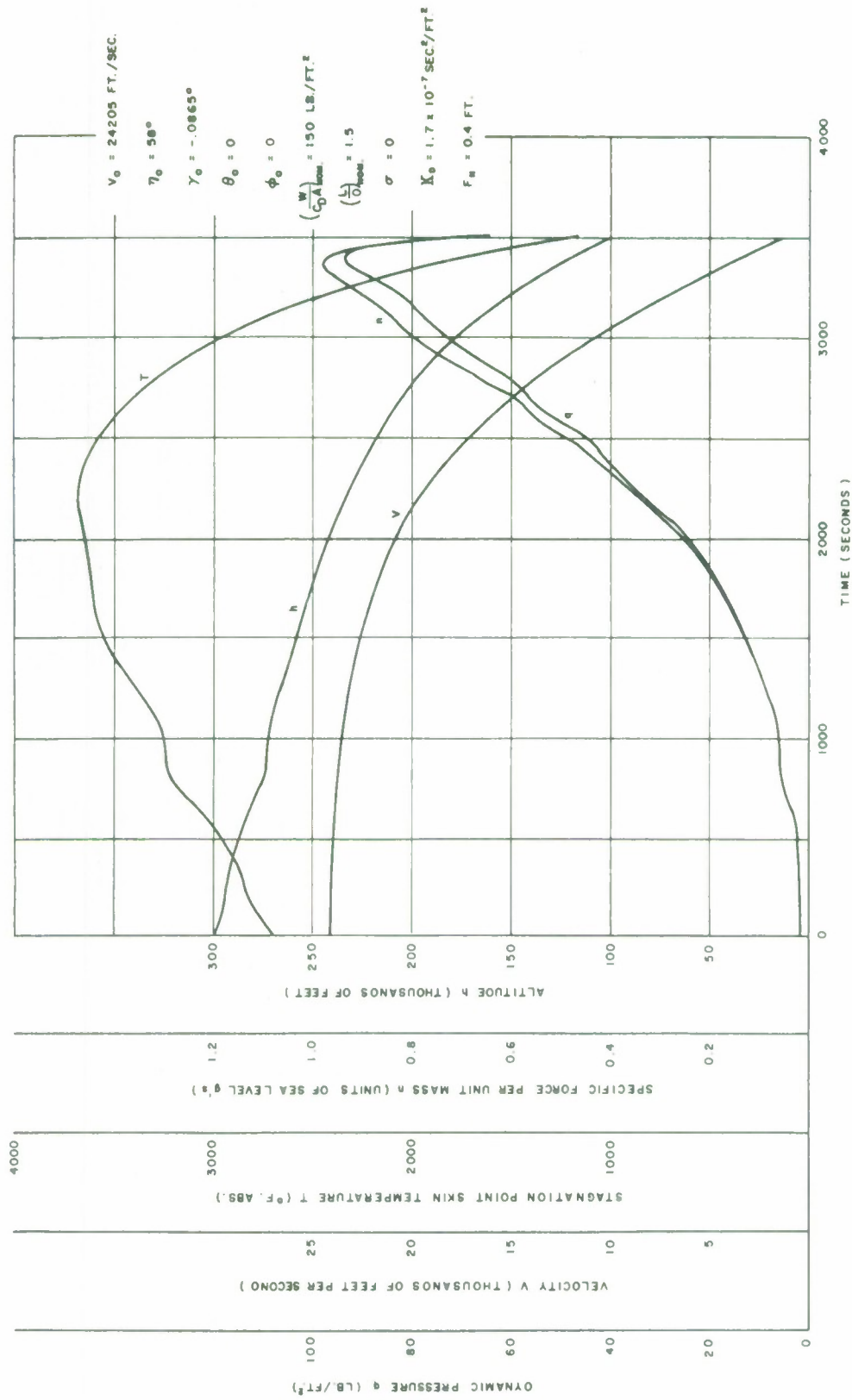
FIG. 9
TYPICAL NEAR-EQUILIBRIUM GLIDE
TRAJECTORY

$V_o = 24205$ FT./SEC.

$\eta_o = 58°$

$\gamma_o = -.0865°$

$\theta_o = 0$

$\phi_o = 0$

$\left(\dfrac{W}{C_D A}\right)_{max} = 150$ LB./FT.^{2}

$\left(\dfrac{L}{D}\right)_{max} = 1.5$

$\sigma = 0$

$K_o = 1.7 \times 10^{-7}$ SEC.^{2}/FT.^{2}

$F_m = 0.4$ FT.

ALTITUDE h (THOUSANDS OF FEET)

SPECIFIC FORCE PER UNIT MASS h (UNITS OF SEA LEVEL g's)

STAGNATION POINT SKIN TEMPERATURE T (°F. ABS.)

VELOCITY V (THOUSANDS OF FEET PER SECOND)

DYNAMIC PRESSURE q (LB./FT.^{2})

TIME (SECONDS)
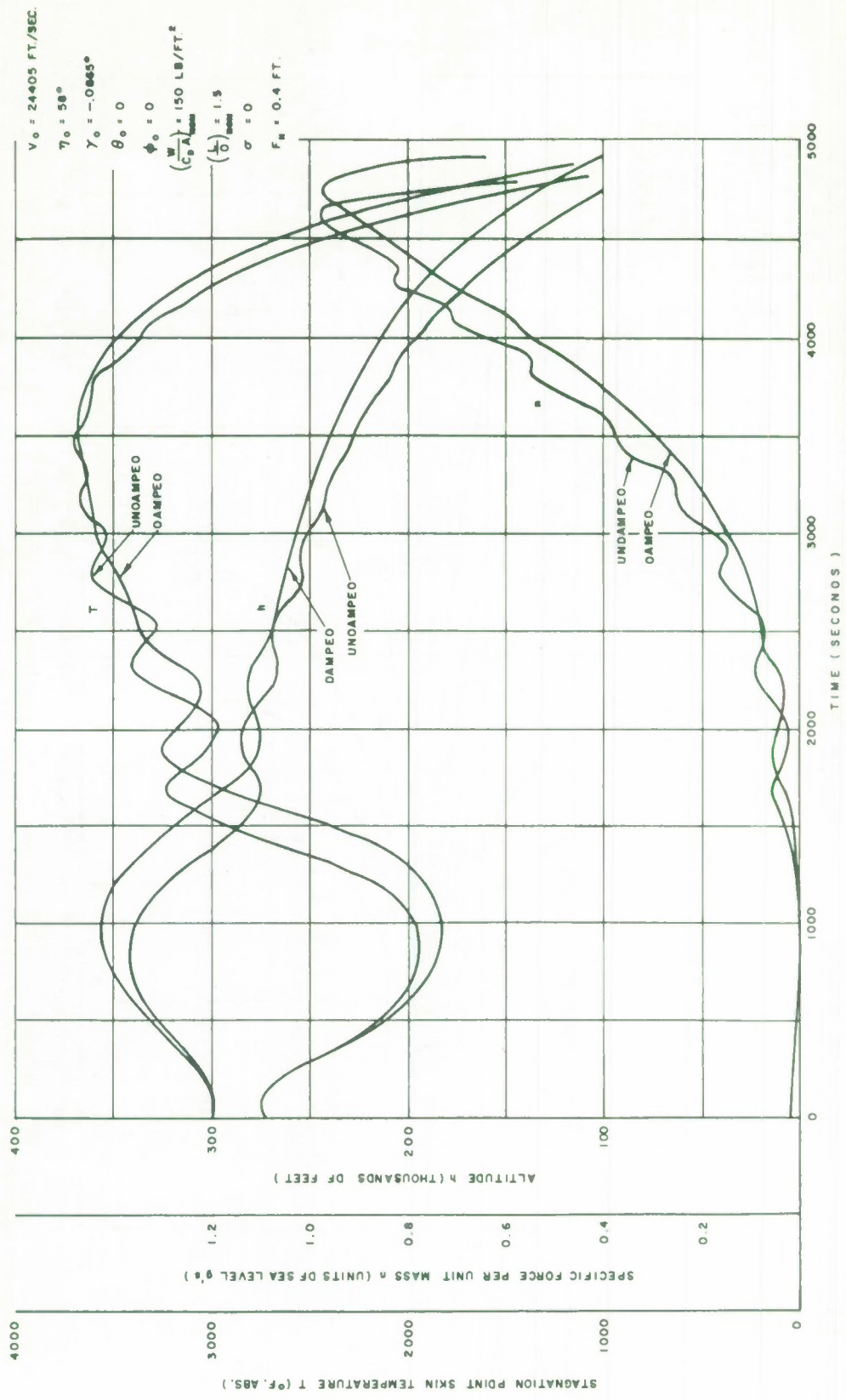
20

EFFECTS OF PHUGOID DAMPING

FIG 10

$V_0 = 24405$ FT/SEC.

$\gamma_0 = 58°$

$\gamma_0 = -0.065°$

$\theta_0 = 0$

$\phi_0 = 0$

$\left(\frac{W}{C_D A}\right)_{max} = 150$ LB/FT^2

$\left(\frac{L}{D}\right)_{max} = 1.5$

$\sigma = 0$

$F_N = 0.4$ FT.

TIME (SECONDS)

ALTITUDE h (THOUSANDS OF FEET)

SPECIFIC FORCE PER UNIT MASS n (UNITS OF SEA LEVEL g's)

STAGNATION POINT SKIN TEMPERATURE T (°F. ABS.)

IB-13.107

21
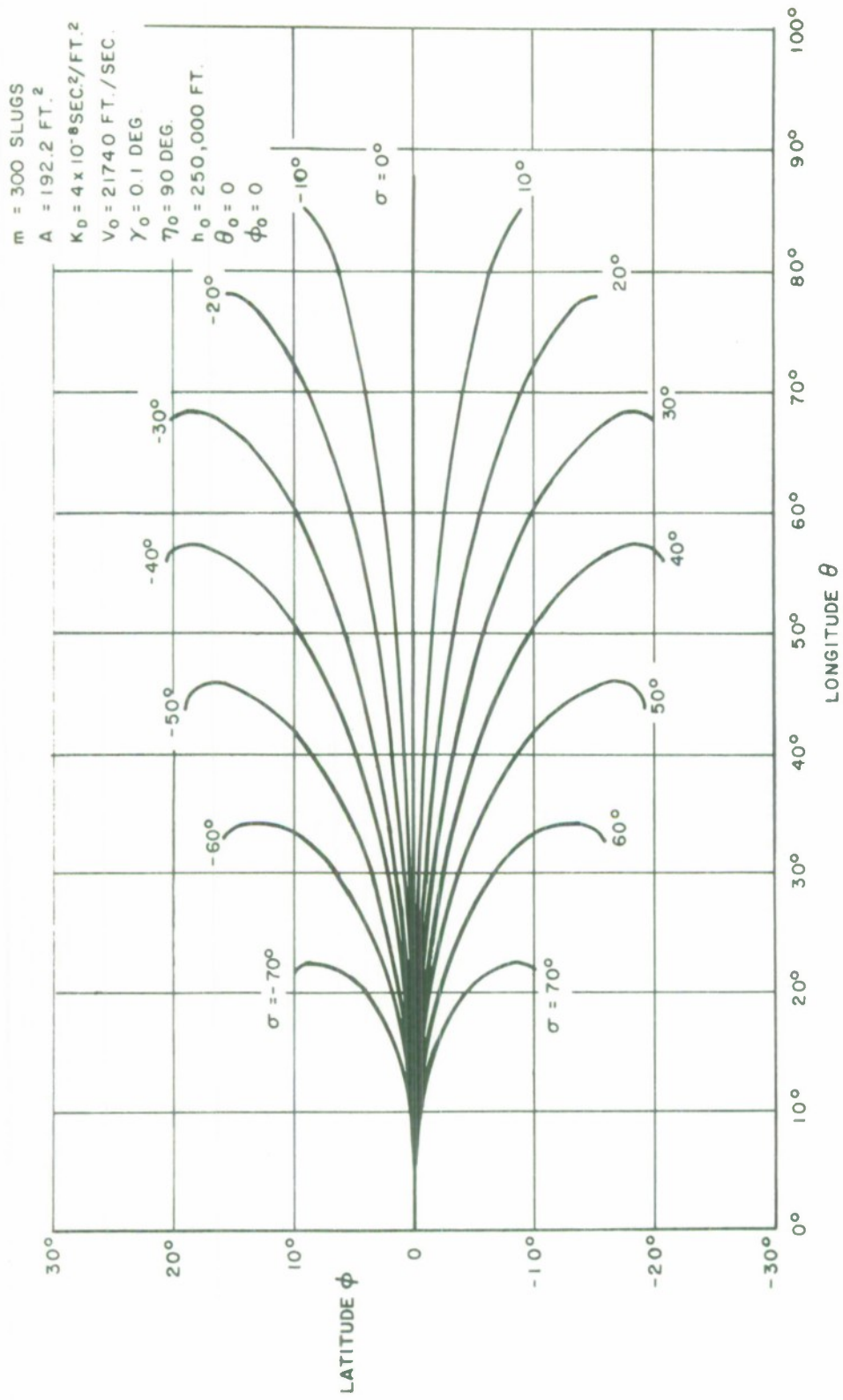
RE-ENTRY TRAJECTORIES FOR VARIOUS BANK ANGLES

$\frac{L}{D} = 2.0$

FIG. 11

IA - 13,315

22
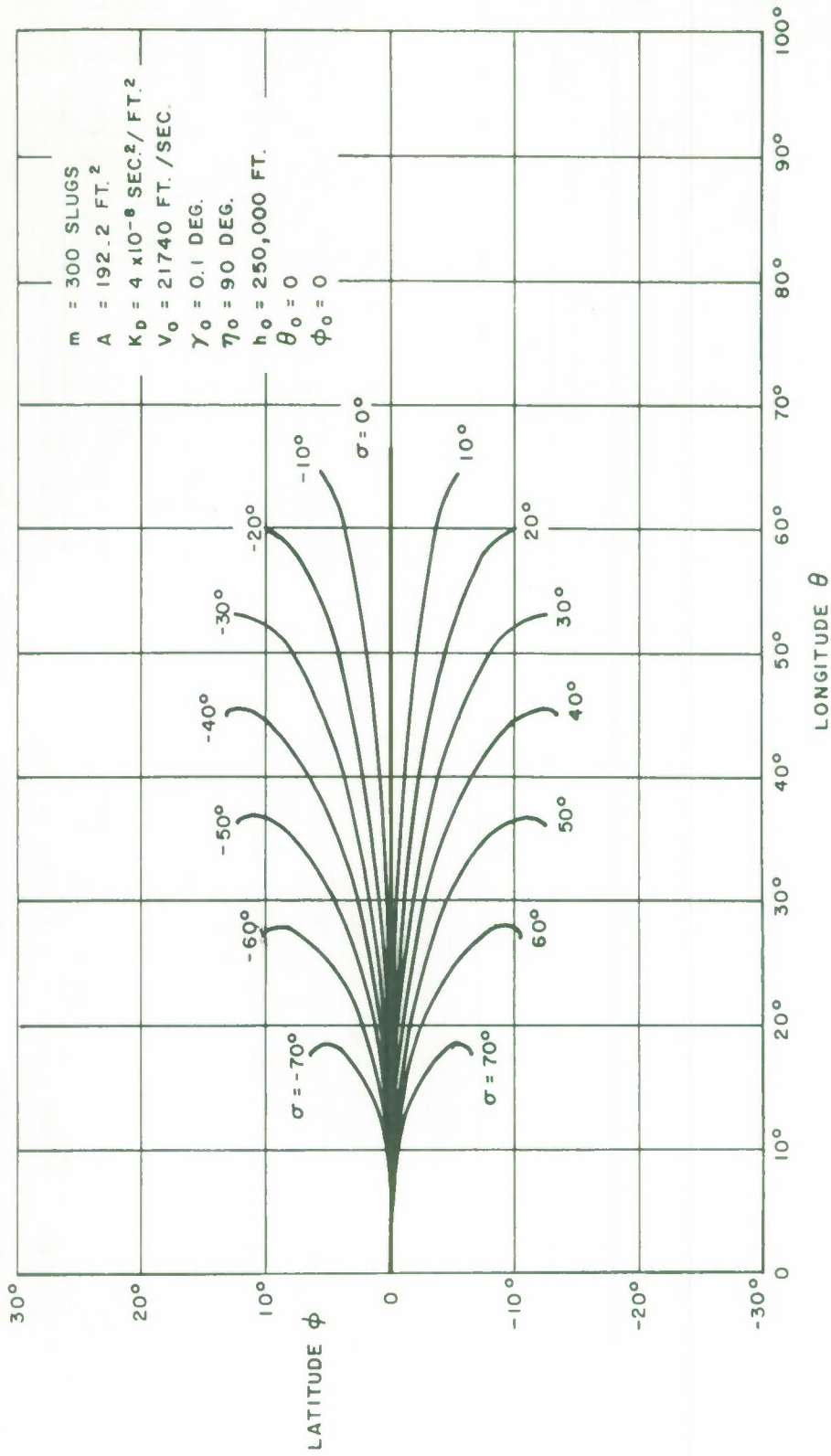
RE-ENTRY TRAJECTORIES FOR VARIOUS BANK ANGLES

$$\frac{L}{D} = 1.5$$

FIG. 12

The plot parameters shown are:

$m = 300$ SLUGS
$A = 192.2$ FT.^{2}
$K_D = 4 \times 10^{-8}$ SEC.^{2}/FT.^{2}
$V_0 = 21740$ FT./SEC.
$\gamma_0 = 0.1$ DEG.
$\eta_0 = 90$ DEG.
$h_0 = 250,000$ FT.
$\theta_0 = 0$
$\phi_0 = 0$

LONGITUDE θ
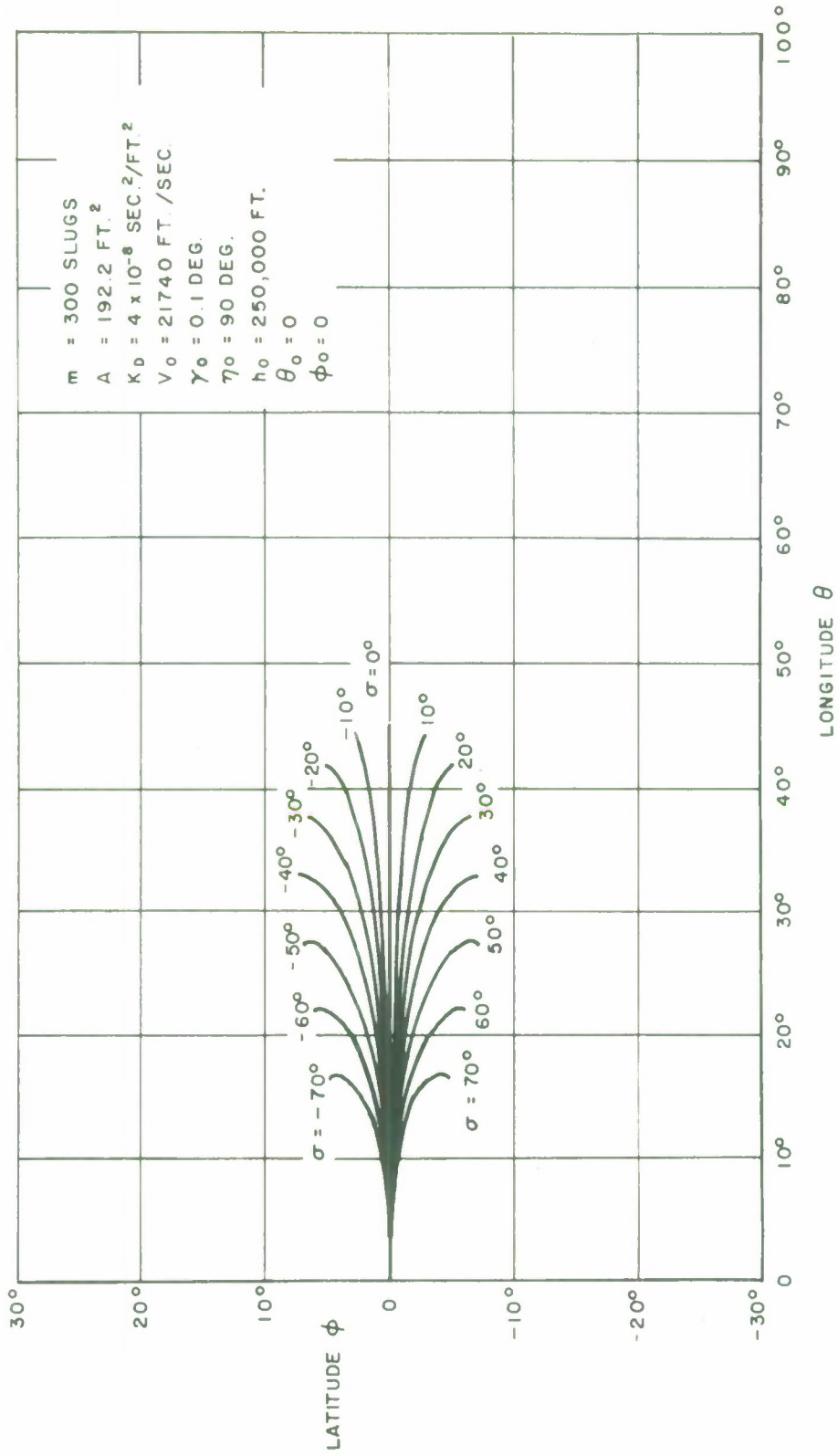
LATITUDE ϕ

RE-ENTRY TRAJECTORIES FOR VARIOUS BANK ANGLES

$\dfrac{L}{D} = 1.0$

FIG. 13

The following parameters are shown on the figure:

$m = 300$ SLUGS
$A = 192.2$ FT.^{2}
$K_D = 4 \times 10^{-8}$ SEC.^{2}/FT.^{2}
$V_0 = 21740$ FT./SEC.
$\gamma_0 = 0.1$ DEG.
$\eta_0 = 90$ DEG.
$h_0 = 250,000$ FT.
$\theta_0 = 0$
$\phi_0 = 0$

LONGITUDE θ

LATITUDE ϕ

natural phugoid oscillation occurs; in the second trajectory, the phugoid
damping ratio is increased to around 0.7 by altitude-rate feedback. The
undesirable temperature and acceleration peaks exhibited along the
uncontrolled trajectory are considerably diminished in the second case.

The trajectories presented so far represent flights at zero
bank angle. All lie essentially in a vertical plane. Figures 11, 12,
and 13, on the other hand, illustrate the lateral maneuvering capability
of a lifting re-entry vehicle when non-zero bank angles are used. In
each case, these figures show projections of vehicle trajectories on the
earth's surface in terms of latitude and longitude. (Alternatively, each
line is the locus of the geocentric sub-vehicle point during re-entry.)
Each trajectory was generated at constant bank angle, with the value
indicated. The trajectories represented in Fig. 11 were made with a
constant L/D of 2.0. Similarly, Figs. 12 and 13 present trajectories
at L/D's of 1.5 and 1.0, respectively.

The vehicle with the maneuvering capability depicted in these
three figures can reach a large area on the earth's surface. If, during
re-entry, bank angle is restricted to values between -70° and $+70^{\circ}$, and
L/D is maintained between 1.0 and 2.0, the "ground area attainable" (GAA)
existing when the vehicle is in its initial state can be estimated by
superimposing Figs. 11, 12, and 13 and drawing the envelope of the points
encompassed. This has been done, and the result is shown in Fig. 14.
By the proper choice of bank angle and L/D, the vehicle is able to reach
any point inside this envelope.

10.2 Digital Results

Figures 15, 16, and 17 illustrate the kind of information the
digital simulation produces. These figures present data on a single
flight of a lifting re-entry vehicle. Aerodynamic characteristics of
this vehicle were identical to those of the vehicle for which the analog
data were derived, but in this case the vehicle's path was controlled by
the re-entry guidance system described in Appendix C. With this guidance
system, the vehicle was able to reach Edwards AFB, California, from a
starting point over the Indian Ocean.

LONGITUDE θ
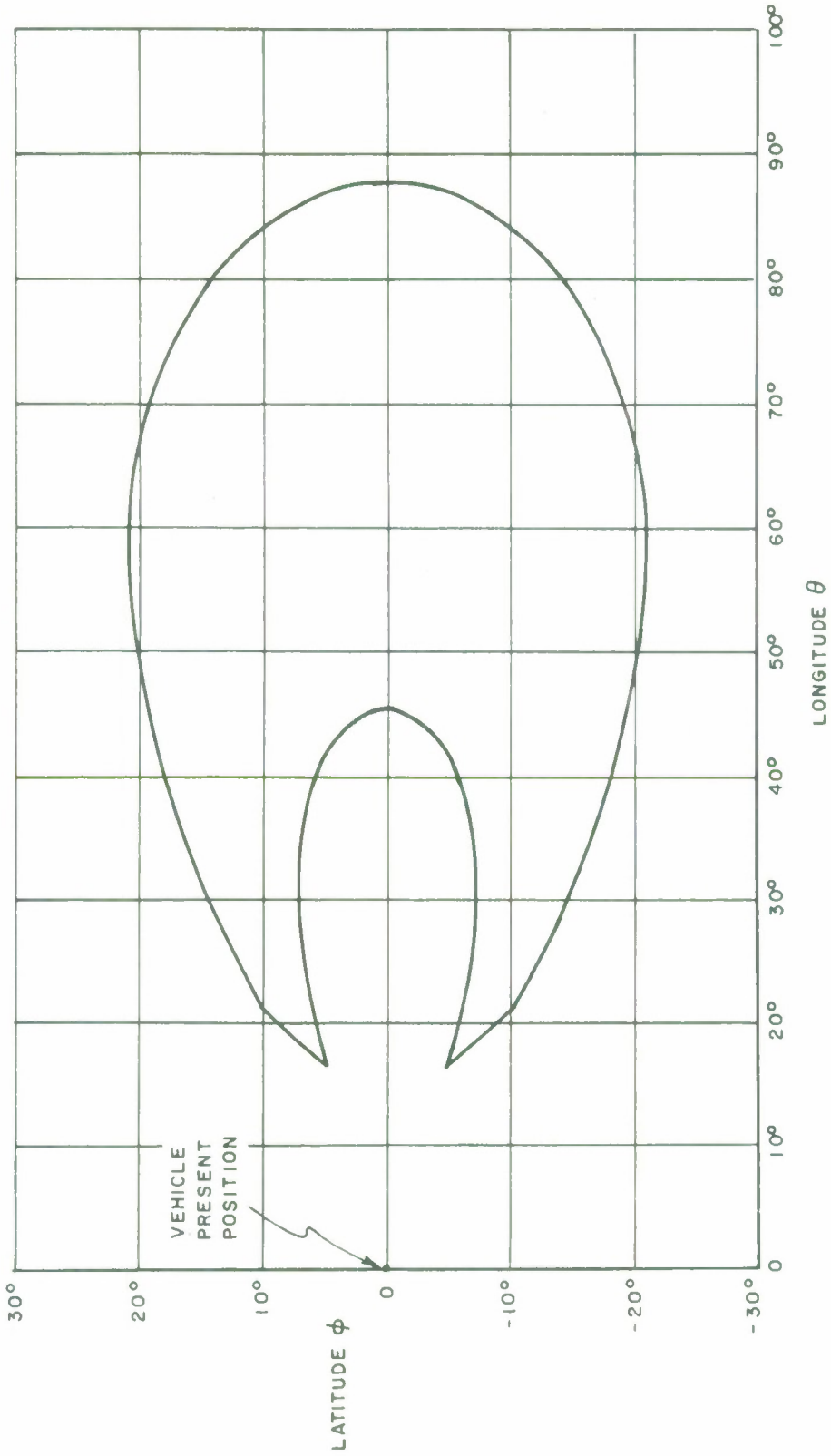
GROUND AREA ATTAINABLE
AT
CONSTANT BANK ANGLE σ
AND
$1.0 \leq \dfrac{L}{D} \leq 2.0$
$-70° \leq \sigma \leq 70°$

FIG. 14
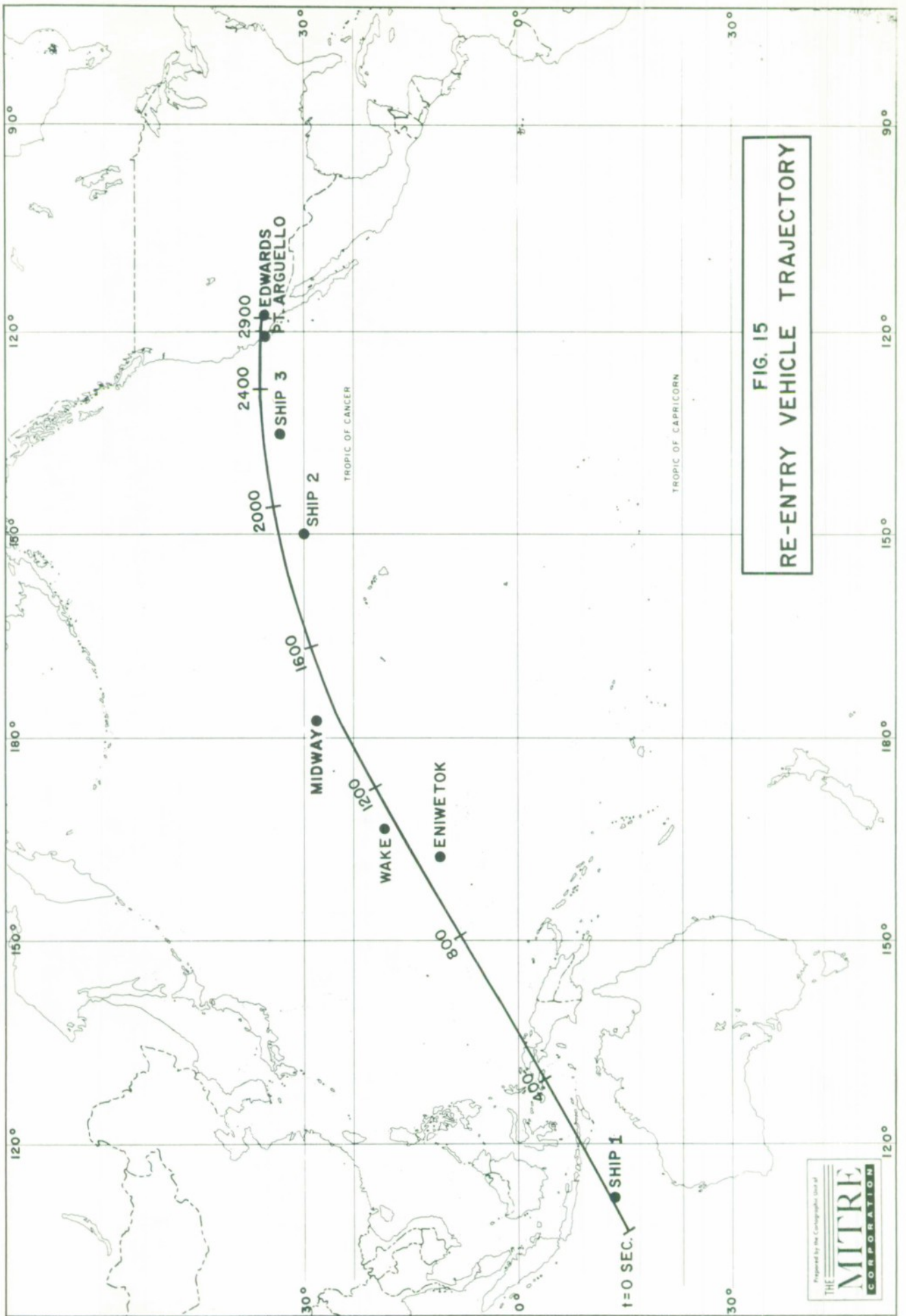
26

FIG. 15
RE-ENTRY VEHICLE TRAJECTORY

HISTORY OF
ALTITUDE, VELOCITY, AND
STAGNATION - POINT SKIN TEMPERATURE

FIG. 16

SHADED AREAS DENOTE
TRACKING PERIODS

TRACKING
STATIONS

SHIP # 1

ENIWETOK

WAKE IS.

MIDWAY IS.

SHIP # 2

SHIP # 3

PT. ARGUELLO

EDWARDS

TIME IN SECONDS

0   400   800   1200   1600   2000   2400   2800
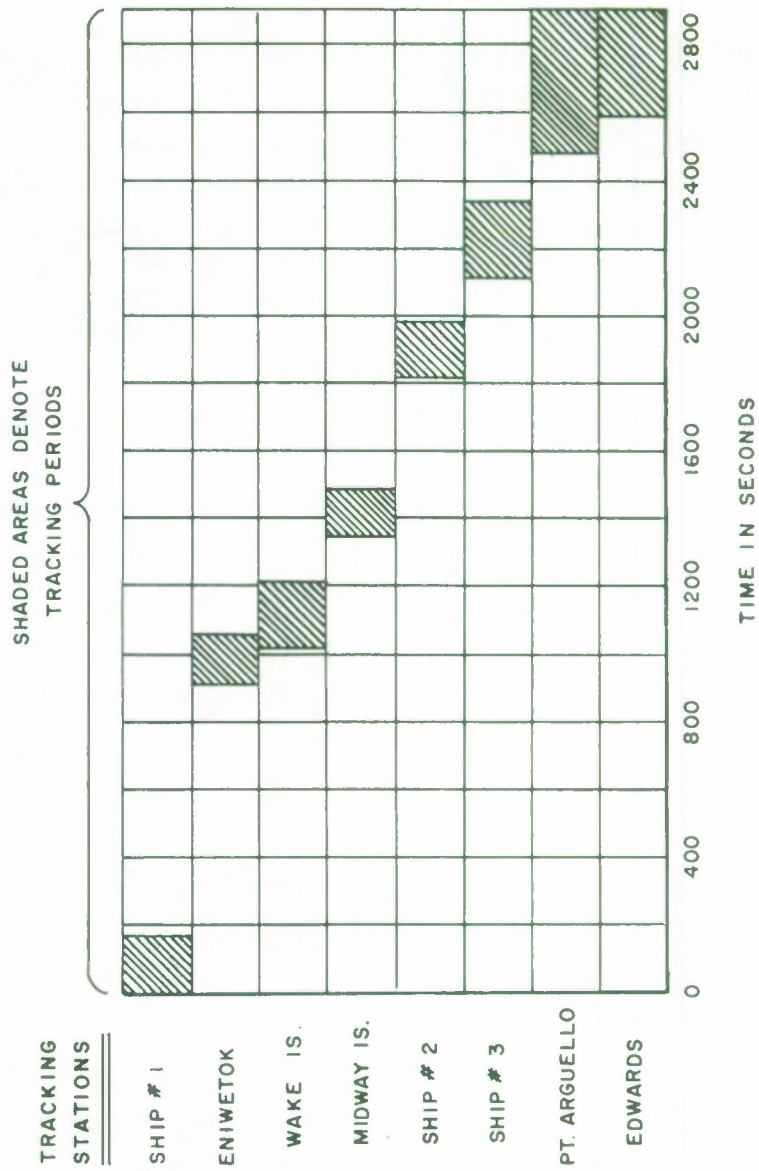
TRACKING HISTORY

FIG. 17

IA - 13,328

29

The horizontal projection of the vehicle's trajectory on the earth is shown in Fig. 15. Time markers along the trajectory permit correlation of the vehicle's geographical position with the altitude, velocity, and skin temperature plotted in Fig. 16. Also shown in Fig. 15 are the locations of eight selected tracking stations along the vehicle's route. In this simulated flight, it was postulated that each station could track the vehicle while the latter was at an elevation angle of 4 degrees or more. The resulting tracking coverage throughout the flight is illustrated in Fig. 17. The figure presents, for each station, a shaded bar indicating the period when the station is able to track. The time scale is the same one used in Figs. 15 and 16. Fig. 17 shows at a glance when the tracking network as a whole is able to collect data, and how many stations are producing data simultaneously at any time.

Figures 15, 16, and 17, taken together, should give the ground system designer a good feel for the fundamental events occurring during this flight, and provide data for quantitative analysis of system requirements. Of course, information on vehicle "g" loads, ground area attainable, tracking station range rates, and other variables is available also, although not included in the figures.

11. CONCLUSIONS

This memorandum has described a computer simulation of re-entry which has been developed for use in the study of ground electronic system requirements. Because of its great flexibility, it can be made to represent the behavior of many different types of re-entry vehicles.

An existing MITRE Corp. simulation, the Flight Trajectory Profile program, produces trajectories of space vehicles throughout the boost and exo-atmospheric phases of flight. Integrating that program and the present re-entry simulation would yield a useful single program capable of simulating complete space missions, from initial booster lift-off to final landing of the re-entry vehicle.

Peter J. Plender

30
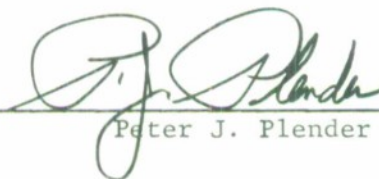
APPENDIX A

Derivation of Equations of Motion

BASIC PRINCIPLE

In vector form, Newton's Second Law of Motion applied to a point mass m is

$$\vec{F} = m\,\frac{d\vec{V}_A}{dt} \quad , \tag{A-1}$$

where $\vec{F}$ represents resultant force and $\vec{V}_A$ is velocity measured with respect to inertial space. The required equations of motion follow directly from this relationship when proper coordinate systems are defined.

COORDINATE SYSTEMS

Coordinate systems have already been defined in the main body of this report. For the purpose of this derivation, however, it will be convenient to use two additional sets of orthogonal reference axes. These axes, an $x_1 y_1 z_1$ set and an $x_2 y_2 z_2$ set, are shown in Fig. A-1. As the figure shows, the $x_1 y_1$ plane is the local horizontal plane; x_1 points northerly and z_1 points downward. The $x_2 y_2 z_2$ axes are oriented with respect to the relative velocity vector $\vec{V}$; x_2 coincides with $\vec{V}$ while y_2 lies in the local horizontal plane. Both sets of axes are right-handed.
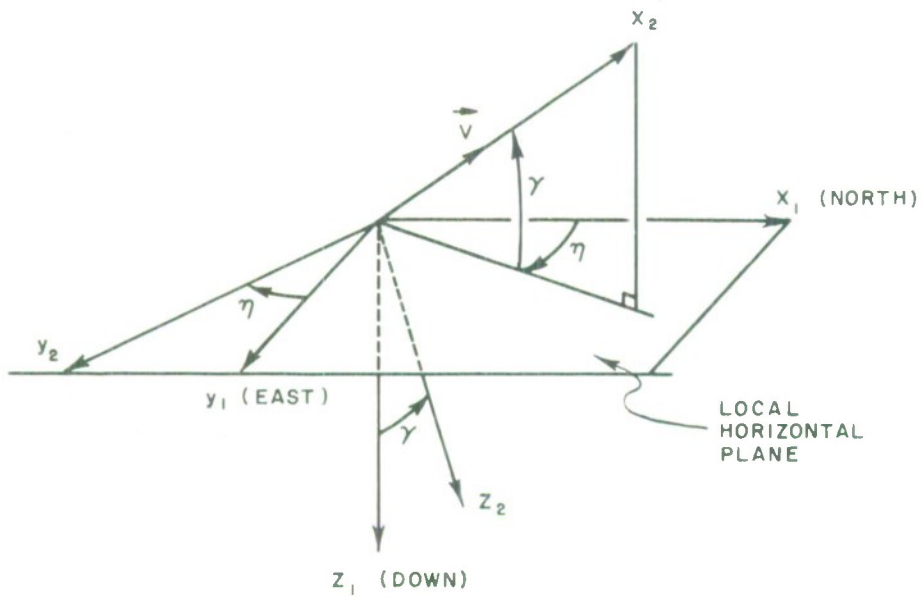
COORDINATE SYSTEMS FOR DERIVATION OF
EQUATIONS OF MOTION

FIG. A-1

FORCES

The vehicle moves under the influence of three forces: gravity, aerodynamic lift, and aerodynamic drag. The latter two forces are defined with respect to wind axes; that is, with respect to axes aligned along and perpendicular to the relative velocity vector $\vec{V}$. It is therefore convenient to expand Eq. A-1 in terms of components in the $x_2 y_2 z_2$ axis system.

The drag force D acts opposite to $\vec{V}$, or along the negative x_2 axis. Vehicle banking occurs around the x_2 axis, and the lift force L is perpendicular to $\vec{V}$. Therefore, L has components in both the y_2 and z_2 directions. In the simple central-force-field model of the earth used here, the gravitational force is directed at the center of the earth coordinate system and has components in the x_2 and z_2 directions. The resultant force vector is the following:

$$\left[\vec{F}\right]_{x_2 y_2 z_2} = \begin{bmatrix} - D - mg \sin \gamma \\ L \sin \sigma \\ - L \cos \sigma + mg \cos \gamma \end{bmatrix} \tag{A-2}$$

The subscript $x_2 y_2 z_2$ denotes that the components given are measured with respect to the $x_2 y_2 z_2$ axis system.

Lift and drag forces depend on dynamic pressure q and the corresponding aerodynamic coefficients:

$$L = q A C_L \tag{A-3}$$

$$D = q A C_D \tag{A-4}$$

A-33

where

$$q = \frac{1}{2} \rho v^2 \qquad\qquad (A-5)$$

and the coefficients C_L and C_D are taken to be functions of angle of
attack only. At the hypersonic velocities existing throughout most of
the re-entry period, neglecting the dependence of C_L and C_D on Mach
number does not introduce serious error.

Gravitational acceleration g is determined by the inverse-square
law,

$$g = \frac{GM}{r^2} \quad , \qquad\qquad (A-6)$$

where GM is the gravitational parameter of the earth.

ACCELERATIONS

Like the forces, the rate of change of $\vec{V}_A$ on the right-hand side
of Eq. A-1 will be expanded into components in the $x_2 y_2 z_2$ axis system.
This axis system moves with the vehicle, and has both translational and
rotational motion. Because of the angular velocity of the reference
axes, the total rate of change of $\vec{V}_A$ is as follows:

$$\left[\frac{d\vec{V}_A}{dt} \right]_{TOTAL} = \left[\frac{d\vec{V}_A}{dt} \right]_{REL.} + \vec{\omega} \times \vec{V}_A \qquad\qquad (A-7)$$

The first term on the right-hand side is the rate of change of $\vec{V}_A$ rela-
tive to the rotating coordinates. The second term is the cross product
of the absolute angular velocity of the coordinate system, $\vec{\omega}$, with $\vec{V}_A$.
Both terms are vectors and, as already stated, are to be evaluated with

A-34

respect to the $x_2y_2z_2$ coordinate system. Reference 6, among others, gives the theoretical basis for Eq. A-7.

The absolute velocity $\vec{V}_A$ can be expressed in terms of the relative velocity V and earth's rate Ω as follows:

$$
\left[\vec{V}_A\right]_{x_2y_2z_2} \equiv \begin{bmatrix} V_{Ax} \\ V_{Ay} \\ V_{Az} \end{bmatrix} = \begin{bmatrix} V + \Omega r \, \text{Cos} \, \varphi \, \text{Sin} \, \eta \, \text{Cos} \, \gamma \\ \Omega r \, \text{Cos} \, \varphi \, \text{Cos} \, \eta \\ \Omega r \, \text{Cos} \, \varphi \, \text{Sin} \, \eta \, \text{Sin} \, \gamma \end{bmatrix} \quad \text{(A-8)}
$$

The subscript $x_2y_2z_2$ denotes that the components given are measured in the $x_2y_2z_2$ system. The right-hand side of Eq. A-8 is a column matrix of the components of the vector $\vec{V}_A$.

Angular velocity of the $x_2y_2z_2$ coordinate system, measured with respect to the $x_1y_1z_1$ axes, is

$$
\left[\vec{\omega}\right]_{x_1y_1z_1} = \begin{bmatrix} \dot{\beta} \, \text{Cos} \, \varphi - \dot{\gamma} \, \text{Sin} \, \eta \\ -\dot{\varphi} + \dot{\gamma} \, \text{Cos} \, \eta \\ -\dot{\beta} \, \text{Sin} \, \varphi + \dot{\eta} \end{bmatrix} \quad \text{(A-9)}
$$

It follows from Fig. A-1 that the corresponding expression for this vector in $x_2y_2z_2$ coordinates can be found by applying the following transformation:

$$
\left[\vec{\omega}\right]_{x_2y_2z_2} = \begin{bmatrix} \text{Cos} \, \eta \, \text{Cos} \, \gamma & \text{Sin} \, \eta \, \text{Cos} \gamma & -\text{Sin} \, \gamma \\ -\text{Sin} \, \eta & \text{Cos} \, \eta & 0 \\ \text{Cos} \, \eta \, \text{Sin} \, \gamma & \text{Sin} \, \eta \, \text{Sin} \gamma & \text{Cos} \, \gamma \end{bmatrix} \left[\vec{\omega}\right]_{x_1y_1z_1}
$$

$$\text{(A-10)}$$

A-35

This transformation leads to an evaluation of $\vec{\omega}$ in the desired reference frame:

$$
\left[\vec{\omega}\right]_{x_2 y_2 z_2} \equiv \begin{bmatrix} \omega_x \\ \omega_y \\ \omega_z \end{bmatrix} = \begin{bmatrix} \dot{\beta}(\cos\varphi\cos\eta\cos\gamma + \sin\varphi\sin\gamma) - \dot{\varphi}\sin\eta\cos\gamma - \dot{\eta}\sin\gamma \\ -\dot{\beta}\cos\varphi\sin\eta - \dot{\varphi}\cos\eta + \dot{\gamma} \\ \dot{\beta}(\cos\varphi\cos\eta\sin\gamma - \sin\varphi\cos\gamma) - \dot{\varphi}\sin\eta\sin\gamma + \dot{\eta}\cos\gamma \end{bmatrix}
$$

$$(A-11)$$

The cross product in Eq. A-7 is equivalent to the following:

$$
\left[\vec{\omega} \times \vec{V}_A\right] = \begin{bmatrix} \omega_y V_{Az} - \omega_z V_{Ay} \\ \omega_z V_{Ax} - \omega_x V_{Az} \\ \omega_x V_{Ay} - \omega_y V_{Ax} \end{bmatrix}
$$

$$(A-12)$$

The absolute rate of change of $\vec{V}_A$ can now be found by using Eqs. A-8, A-11, and A-12 to carry out the operations specified in Eq. A-7. The lengthly results thus obtained can be simplified considerably by the use of the following identities:

$$
r\,\dot{\theta}\,\cos\varphi\,\sin\eta + r\,\dot{\varphi}\,\cos\eta = V\cos\gamma \qquad (A-13)
$$

$$
r\,\dot{\theta}\,\cos\varphi\,\cos\eta - r\,\dot{\varphi}\,\sin\eta = 0 \qquad (A-14)
$$

$$
\dot{r} = V\sin\gamma \qquad (A-15)
$$

The angular rate $\dot{\beta}$ can be eliminated from the equations by noting that it is equal to $\dot{\theta}$ plus the earth's inertial rotational rate:

$$
\dot{\beta} = \dot{\theta} + \Omega \qquad (A-16)
$$

A-36

The desired result is

$$
\left[\frac{d\vec{V}_A}{dt}\right]_{x_2 y_2 z_2} =
\begin{bmatrix}
\dot{V} + \Omega^2 r \, \text{Cos}\, \varphi \, [\text{Sin}\, \varphi \, \text{Cos}\, \eta \, \text{Cos}\, \gamma - \text{Cos}\, \varphi \, \text{Sin}\, \gamma] \\[2ex]
V\text{Cos}\gamma[\dot{\eta} - \dfrac{V}{r} \, \text{Tan}\, \varphi \, \text{Sin}\, \eta \, \text{Cos}\, \gamma] \\
\quad + 2\Omega V[\text{Cos}\, \varphi \, \text{Cos}\, \eta \, \text{Sin}\, \gamma - \text{Sin}\, \varphi \, \text{Cos}\, \gamma] \\
\quad - \Omega^2 \, r \, \text{Sin}\, \varphi \, \text{Cos}\, \varphi \, \text{Sin}\, \eta \\[2ex]
V[\dfrac{V}{r} \, \text{Cos}\, \gamma - \dot{\gamma}] + 2\Omega V \, \text{Cos}\, \varphi \, \text{Sin}\, \eta \\
\quad + \Omega^2 r \, \text{Cos}\, \varphi \, [\text{Sin}\, \varphi \, \text{Cos}\, \eta \, \text{Sin}\, \gamma + \text{Cos}\, \varphi \, \text{Cos}\, \gamma]
\end{bmatrix}
\quad (A\text{-}17)
$$

FINAL EQUATIONS OF MOTION

Three final equations of motion result when Eqs. A-2 and A-17 are substituted into Eq. A-1 and corresponding components of this vector equation are set equal to each other:

$$
\dot{V} = -\frac{D}{m} - g \, \text{Sin}\, \gamma - \Omega^2 r \, \text{Cos}\, \varphi \, [\text{Sin}\varphi\text{Cos}\eta\text{Cos}\gamma - \text{Cos}\varphi\text{Sin}\gamma] \quad (A\text{-}18)
$$

$$
\dot{\eta} = \frac{L \, \text{Sin}\, \sigma}{mV \, \text{Cos}\, \gamma} + \frac{V}{r} \, \text{Tan}\, \varphi \, \text{Sin}\, \eta \, \text{Cos}\, \gamma
$$

$$
- 2\Omega[\text{Cos}\, \varphi \, \text{Cos}\, \eta \, \text{Tan}\, \gamma - \text{Sin}\, \varphi] \quad (A\text{-}19)
$$

$$
+ \frac{\Omega^2 r \, \text{Sin}\, \varphi \, \text{Cos}\, \varphi \, \text{Sin}\, \eta}{V \, \text{Cos}\, \gamma}
$$

$$
\dot{\gamma} = \frac{L \, \text{Cos}\, \sigma}{mV} - \left[\frac{g}{V} - \frac{V}{r}\right] \text{Cos}\, \gamma + 2\Omega \, \text{Cos}\, \varphi \, \text{Sin}\, \eta
$$

$$
(A\text{-}20)
$$

$$
+ \frac{\Omega^2 r \, \text{Cos}\, \varphi}{V} \, [\text{Sin}\, \varphi \, \text{Cos}\, \eta \, \text{Sin}\, \gamma + \text{Cos}\, \varphi \, \text{Cos}\, \gamma]
$$

A-37

Since these are first-order differential equations, only three integrations are involved. Three more integrations are required before the complete solution can be obtained. These are provided by the following kinematic equations:

$$\dot{r} = V \sin \gamma \tag{A-21}$$

$$\dot{\varphi} = \frac{V}{r} \cos \eta \cos \gamma \tag{A-22}$$

$$\dot{\theta} = \frac{V \sin \eta \cos \gamma}{r \cos \varphi} \tag{A-23}$$

Eqs. A-18 through A-23 constitute the complete set of equations of motion.

Lastly, it is evident from the geometry of the problem that vehicle altitude is determined by the relation

$$h = r - R_e \tag{A-24}$$

APPENDIX B

Deviation of Closed-Form Prediction Equations for
Lifting Re-entry Trajectories

EQUILIBRIUM GLIDE TRAJECTORY

The closed-form trajectory prediction equations to be developed here are based on the so-called "equilibrium glide". This type of trajectory is defined as one along which the centrifugal and vertical lift forces on the vehicle exactly counterbalance the gravitational force. One of the principal merits of the equilibrium glide is that it can be described by relatively simple analytical relationships.

HORIZONTAL RANGE PREDICTION

If two of the equations of motion derived in Appendix A (Eqs. A-18 and A-20) are written in terms of coordinates fixed to a non-rotating earth model, they become the following:

$$\dot{V}_A = - \frac{D}{m} - g \, \text{Sin} \, \gamma_A \tag{B-1}$$

$$\dot{\gamma}_A = \frac{L \, \text{Cos} \, \sigma_A}{m \, V_A} + \frac{V_A \, \text{Cos} \, \gamma_A}{r} - \frac{g \, \text{Cos} \, \gamma_A}{V_A} \tag{B-2}$$

where the relative velocity V has been transformed to absolute velocity V_A, and a flight path angle γ_A is defined as the angle of the vector $\vec{V}_A$ above the local horizontal. The bank angle σ_A is defined with respect to a vertical plane containing $\vec{V}_A$. Now, the equilibrium glide is the path for which $\dot{\gamma}_A = 0$. That is,

$$\frac{L \, \text{Cos} \, \sigma_A}{m \, V_A} = \frac{g \, \text{Cos} \, \gamma_A}{V_A} - \frac{V_A \, \text{Cos} \, \gamma_A}{r} \tag{B-3}$$

B-39

and there is equilibrium between lift, gravity, and centrifugal forces. If flight path angle γ_A is restricted to small values, so that $\cos \gamma_A \approx 1$, this equation is equivalent to

$$\frac{L \cos \sigma_A}{mg} = 1 - \frac{V_A^2}{gr} \tag{B-4}$$

The quantity gr is equal to V_c^2, the square of the velocity of a satellite in circular orbit at radius r. Therefore, Eq. B-4 can be written as

$$\frac{L \cos \sigma_A}{mg} = 1 - \left(\frac{V_A}{V_c}\right)^2 \tag{B-5}$$

Clearly, the ratio $\dfrac{V_A}{V_c}$ must be less than 1 if the vertical lift component, $L \cos \sigma_A$, is to act in the upward direction.

With the assumption that the flight conditions are such that $g \sin \gamma_A \ll \dfrac{D}{m}$, Eq. B-1 can be simplified to the following:

$$\dot{V}_A = -\frac{D}{m} \tag{B-6}$$

This equation can be combined with B-5 to produce a useful range prediction result when velocity is related to horizontal distance traveled. For small values of γ_A,

$$\frac{dS}{dt} = V_A \cos \gamma_A = \approx V_A \tag{B-7}$$

Where dS is the differential horizontal distance traveled in time dt. It follows that

$$\dot{V}_A = \frac{dV_A}{dt} = \frac{dS}{dt} \quad \frac{dV_A}{dS} = V_A \frac{dV_A}{dt} \tag{B-8}$$

When combined, equations B-5, B-6, and B-8 yield the result

$$V_A \frac{dV_A}{dS} = - \frac{g}{(L/D) \cos \sigma_A} \left[1 - \frac{V_A^2}{V_c^2} \right] \tag{B-9}$$

This differential equation in V_A can be integrated in closed form if $\frac{L}{D} \cos \sigma_A$, g, and V_c are held constant. The latter two variables actually vary very little during lifting re-entry of the earth's atmosphere. The quantity $\frac{L}{D} \cos \sigma_A$ is controllable, and can be held fixed arbitrarily. The result of integrating Eq. B-9 between the velocity limits V_A and zero and the distance limits zero and S is

$$S = - \frac{r_{AV.}}{2} \left(\frac{L}{D} \right) \cos \sigma_A \ln \left[1 - \frac{V_A^2}{V_c^2} \right] \tag{B-10}$$

where $r_{AV.} \equiv \frac{V_c^2}{g}$ = Average value of radius during flight. The minus sign is consistent with the requirement that initial re-entry velocity be sub-circular, so that $0 < \frac{V_A}{V_c} < 1$ and the logarithm on the right hand side is always negative. This equation gives the approximate horizontal distance traveled by a lifting re-entry vehicle on an equilibrium glide trajectory with constant $\frac{L}{D} \cos \sigma_A$, from the point at which inertial velocity is V_A.

In the special case for which $\sigma_A = 0$, approximate horizontal distance is

$$S = - \frac{r_{AV.}}{2} \left(\frac{L}{D} \right) \ln \left[1 - \frac{V_A^2}{V_c^2} \right] \tag{B-11}$$

The projection of this trajectory on the surface of the earth is a great

B-41

circle which subtends an angle λ approximately equal to $\left| \dfrac{S}{r_{AV.}} \right|$. Therefore,

$$\lambda = -\frac{1}{2} \left(\frac{L}{D} \right) \ell n \left[1 - \frac{V_A^2}{V_c^2} \right] \tag{B-12}$$

ALTITUDE RATE

In this section, a simple expression for altitude rate during an equilibrium glide will be developed from the basic equations of motion and an analytical model of the atmosphere.

Altitude rate can best be evaluated indirectly, by writing it as follows:

$$\frac{dh}{dt} = \frac{\left[\dfrac{dV_A}{dt} \right]}{\left[\dfrac{dV_A}{dh} \right]} \tag{B-13}$$

The problem thus becomes one of evaluating the derivations $\dfrac{dV_A}{dt}$ and $\dfrac{dV_A}{dh}$.

An approximation for $\dfrac{dV_A}{dt}$ has already been given in Eq. B-6:

$$\frac{dV_A}{dt} = -\frac{D}{m} \tag{B-14}$$

The derivative $\dfrac{dV_A}{dh}$ can be derived from the basic equation of the flight path, Eq. B-5.

The aerodynamic lift force L in this equation is given by the expression

$$L = \frac{1}{2} \rho V^2 A C_L \quad , \tag{B-15}$$

B-42

where V is the velocity of the vehicle relative to the earth's rotating atmosphere. The velocities V and V_A differ by a maximum of about 1500 feet per second at the equator and less at other latitudes — a relatively small percentage difference during most of the re-entry glide. As an approximation, therefore, V_A can be used for V, and Eq. B-5 becomes

$$\frac{\rho V_A^2 A C_L \cos \sigma_A}{2 mg} = 1 - \left(\frac{V_A}{V_c}\right)^2 \tag{B-16}$$

By taking logarithms of both sides of this equation and differentiating with respect to altitude h while holding $\dfrac{A C_L \cos \sigma_A}{mg}$ and V_c constant, the following result is obtained:

$$\frac{1}{\rho}\frac{d\rho}{dh} + \frac{2}{V_A}\frac{dV_A}{dh} = \frac{-2V_A}{V_c^2 \left[1 - \left(\dfrac{V_A}{V_c}\right)^2\right]} \quad \frac{dV_A}{dh} \tag{B-17}$$

By the use of Eq. B-5, this can be simplified as follows:

$$\frac{dV_A}{dh} = -\frac{V_A}{2}\left[\frac{L \cos \sigma_A}{mg}\right]\frac{1}{\rho}\frac{d\rho}{dh} \tag{B-18}$$

In evaluating the right-hand derivative in this equation, it is convenient to use the exponential model atmosphere:

$$\rho = \rho_{SL}\ e^{-kh} \tag{B-19}$$

It can be verified that by virtue of this relationship between density and altitude, the following is true:

$$\frac{1}{\rho} \frac{d\rho}{dh} = -k \tag{B-20}$$

Therefore, the derivative $\dfrac{dV_A}{dh}$ (Eq. B-18) becomes

$$\frac{dV_A}{dh} = \frac{kV_A}{2} \quad \frac{L \cos \sigma_A}{mg} \tag{B-21}$$

With the substitution of this derivative and the one of Eq. B-14 into Eq. B-13, altitude rate is found to be

$$\frac{dh}{dt} = \frac{-\dfrac{D}{m}}{\dfrac{kV_A \ L \cos \sigma_A}{2 \ mg}} \tag{B-22}$$

or

$$\boxed{\frac{dh}{dt} = - \frac{2g}{kV_A \left(\dfrac{L}{D} \right) \cos \sigma_A}} \tag{B-23}$$

PREDICTION OF REMAINING TIME OF FLIGHT

Equation B-7 provides a simple means for determining the time of flight remaining at any instant:

$$dt \approx \frac{dS}{V_A} \tag{B-24}$$

By combining Eq. B-9 with this one, the following equation in t and V_A can be obtained:

$$\int_0^{t_F} dt = - \int_{V_A}^{0} \left(\frac{L}{D} \right) \frac{\cos \sigma_A}{g} \quad \frac{dV_A}{\left[1 - \dfrac{V_A^2}{V_c^2} \right]} \tag{B-25}$$

B-44

If the indicated integrations are carried out, with $\left[\dfrac{L}{D} \dfrac{\text{Cos } \sigma_A}{g} \right]$ and V_c held constant, the time of flight remaining at the instant when velocity is V_A is found to be

$$
t_F = \frac{V_c}{2g} \left(\frac{L}{D} \right) \text{Cos } \sigma_A \; \ell n \left[\frac{1 + \dfrac{V_A}{V_c}}{1 - \dfrac{V_A}{V_c}} \right] \tag{B-26}
$$

APPENDIX C

Guidance System for Lifting Re-entry Vehicle

<u>SCOPE</u>

This appendix describes a system for guiding a lifting re-entry vehicle, such as the X-20 glider, to a desired destination on the earth with high probability of success. This system is only one of many possibilities. It differs from the one actually used in the X-20, but is very similar, in concept and in many details, to the energy management system described in Ref. 2. Basically, it is designed to control the locus of possible landing points.

Re-entry of a maneuverable vehicle like the X-20 is a process involving several distinct phases. While the vehicle is still out of the atmosphere, its path is ballistic, and the only control exercised is that of vehicle attitude. When aerodynamic forces develop, the trajectory becomes controllable and a second phase, the glide phase, begins. It is during this phase that the critical problems of energy management occur. When the vehicle nears its destination and most of its initial energy has been dissipated, control of the vehicle passes to a terminal guidance system, and the last phase begins. This transition occurs at an altitude of approximately 100,000 feet, where velocity is on the order of 4000 feet per second. The terminal guidance system, which may be a human pilot using visual cues, flight instruments and advisory information radioed from the ground, has the job of landing the vehicle safely in a designated recovery area.

The guidance system described here is designed to carry the vehicle through the second phase of re-entry. Simulations using this guidance system ordinarily end when an altitude of 100,000 feet is reached, since this mode of flight is not valid beyond that point.

GUIDANCE CONCEPT

Two broad categories of re-entry guidance systems have been proposed and studied in recent years. These are the prediction-type systems and the systems designed to guide the vehicle onto a pre-computed, reference trajectory. The present scheme belongs in the first category. It is based on the concept of the "ground area attainable" (GAA) or "footprint" of a maneuverable re-entry vehicle. The GAA is defined as the ground area to which the vehicle is capable of maneuvering from its existing state of position and velocity. In Fig. C-1, the GAA is shown with respect to the re-entry vehicle in a plan view which neglects the earth's curvature. The intended destination on the ground is shown at an arbitrary position inside the GAA boundary.

As the vehicle descends through the atmosphere and its velocity decreases, the GAA shrinks in size and changes shape slightly. In order for the vehicle to reach a given destination, that destination must be kept within the diminishing GAA. From an alternate point of view, the GAA must be controlled by vehicle maneuvering so that it always covers the desired destination.

The present guidance system is designed to drive the GAA continuously to the position in which the desired destination is exactly in the center.
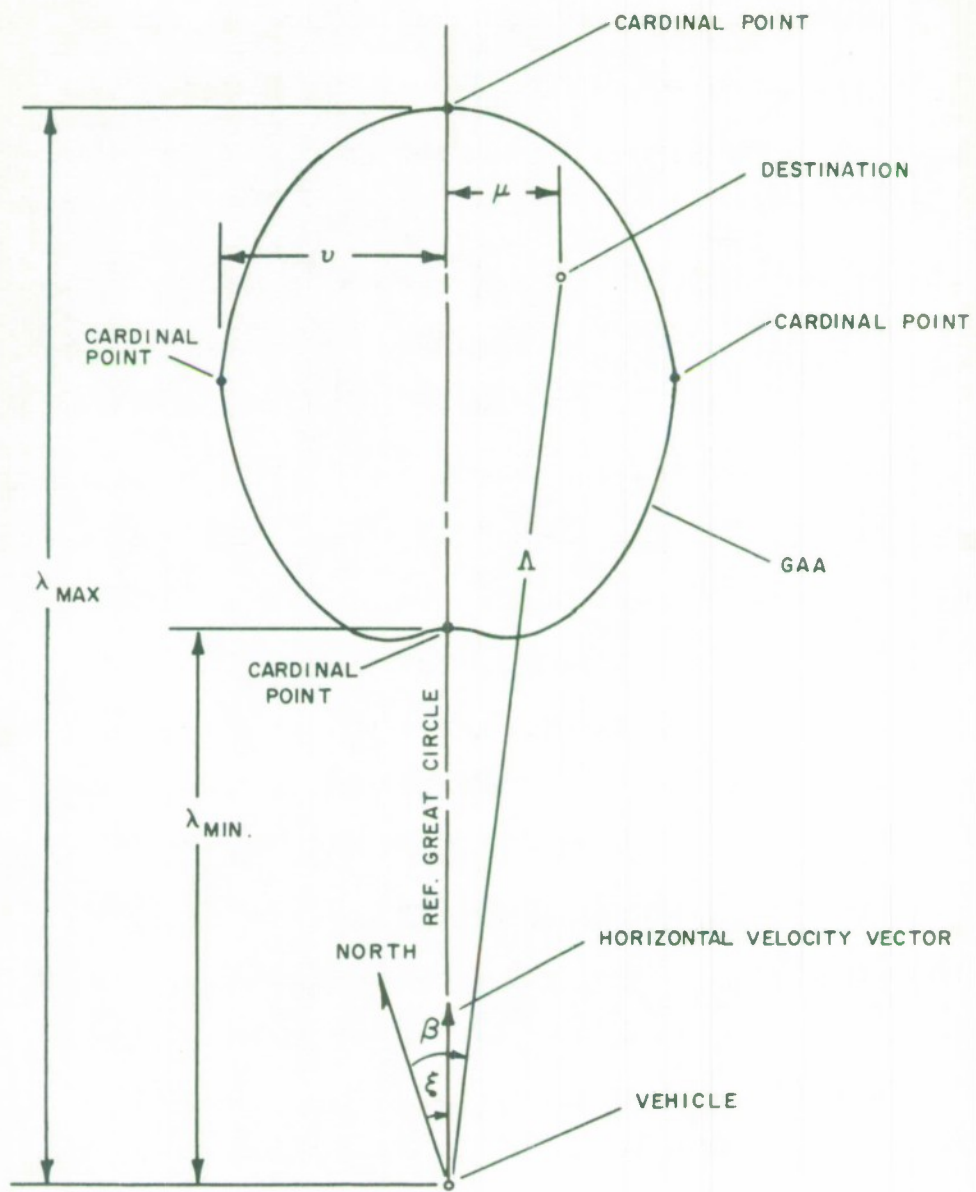
GROUND AREA ATTAINABLE

FIG. C-1

With the target point ideally centered in the GAA, random perturbations of the trajectory, produced by such real factors as guidance equipment errors and vehicle system malfunctions causing temporary loss of guidance or control, have the least effect on the ability of the vehicle to reach that point.

Another feature of this guidance scheme is its use of the equilibrium glide trajectory as a basis for computing the maneuvering capability of the vehicle at any instant. The GAA at any time is determined by calculating the limits to which the vehicle could travel on equilibrium glide trajectories. These limits are not the absolute limits achievable by optimum programming of the guidance commands, but are the limits which can be realized with the present guidance system.

The two basic guidance commands are lift-to-drag ratio $(\frac{L}{D})$ and bank angle σ. Both are based on the computed position of the target point with respect to the four cardinal points of the GAA. The latter points are determined by means of approximate, closed-form equations. Figure C-1 shows the cardinal point locations.

GAA CARDINAL POINTS

The desired landing point and the GAA cardinal points are specified with respect to a particular reference line on a non-rotating spherical earth. This line is the great circle contained in the plane passed through the center of the earth and the vehicle's instantaneous velocity vector. The closest and most distant cardinal points, lying on the reference great circle, are reached with zero bank angle. By virtue of the

results derived in Appendix B (Eq. B-12), equilibrium glide trajectories from the present position to these points cover the following central angles:

Minimum range:

$$\lambda_{MIN.} = -\frac{1}{2} \left(\frac{L}{D}\right)_{MIN.} \ln\left[1 - \frac{V_A^2}{V_c^2}\right] \tag{C-1}$$

Maximum range:

$$\lambda_{MAX.} = -\frac{1}{2} \left(\frac{L}{D}\right)_{MAX} \ln\left[1 - \frac{V_A^2}{V_c^2}\right] \tag{C-2}$$

where

$$V_c^2 = gr = \frac{GM}{r} ,$$

and V_A is the velocity of the vehicle with respect to inertial space. In terms of the variables used in the equations of motion, the magnitude of V_A is

$$V_A = \sqrt{V^2 + 2\Omega\, rV\, Cos\, \varphi\, Sin\, \eta\, Cos\, \gamma + (\Omega r\, Cos\, \varphi)^2} \tag{C-3}$$

Similarly, the central angle from each lateral cardinal point to the reference great circle is approximately as follows:

$$\nu = 0.160 \left(\frac{L}{D}\right)_{MAX.}^{1.19} \left[\frac{V_A}{V_c}\right]^{2.19} \tag{C-4}$$

C-51

This last relationship was derived empirically from re-entry trajectories produced by an analog computer. It is valid for values of $\frac{L}{D}$ between 1.0 and 2.0 and for values of $\frac{V_A}{V_c}$ between 0.2 and 0.9.

These prediction equations (C-1, C-2, and C-4) are reasonably accurate when applied to the non-rotating reference frame in which they were derived.

POSITION OF DESIRED DESTINATION

As illustrated in Fig. C-1, the position of the destination is defined by two central angles: Λ, the one between the destination and the vehicle, and μ, the one subtended by the great circle arc passing through the destination and intersecting the reference great circle at right angles. These central angles are defined with respect to a non-rotating reference sphere with center at the center of the earth. In Fig. C-1, the position of the destination with respect to this reference system is the position it occupies at the end of the vehicle's flight.

By analyzing the spherical geometry involved, with the aid of Figs. C-1 and C-2, it can be shown that

$$\Lambda = \text{Cos}^{-1} \left[\text{Sin } \varphi_T \text{ Sin } \varphi + \text{Cos } \varphi_T \text{ Cos } \varphi \text{ Cos } (\theta_{T_F} - \theta) \right] \quad \text{(C-5)}$$

and

$$\mu = \text{Sin}^{-1} \left[\text{Sin } \Lambda \text{ Sin } (\beta - \xi) \right] \quad \text{(C-6)}$$

where

$$\beta = \text{Sin}^{-1} \left[\frac{\text{Cos } \varphi_T \text{ Sin } (\theta_{T_F} - \theta)}{\text{Sin } \Lambda} \right] \quad \text{(C-7)}$$

$$\xi = \text{Tan}^{-1} \left[\frac{V \text{ Cos } \gamma \text{ Sin } \eta + \Omega \text{ r Cos } \varphi}{V \text{ Cos } \gamma \text{ Cos } \eta} \right] \quad \text{(C-8)}$$

C-52

NORTH
AXIS

PRESENT POSITION OF
DESTINATION $[\phi_T, \theta_T]$

FINAL POSITION OF
DESTINATION $[\phi_T, \theta_T + \Omega t_F]$

$\Delta\theta_T = \Omega t_F$

Λ

PRESENT VEHICLE
POSITION $[\phi, \theta]$

NON-ROTATING
EARTH REFERENCE
SPHERE.
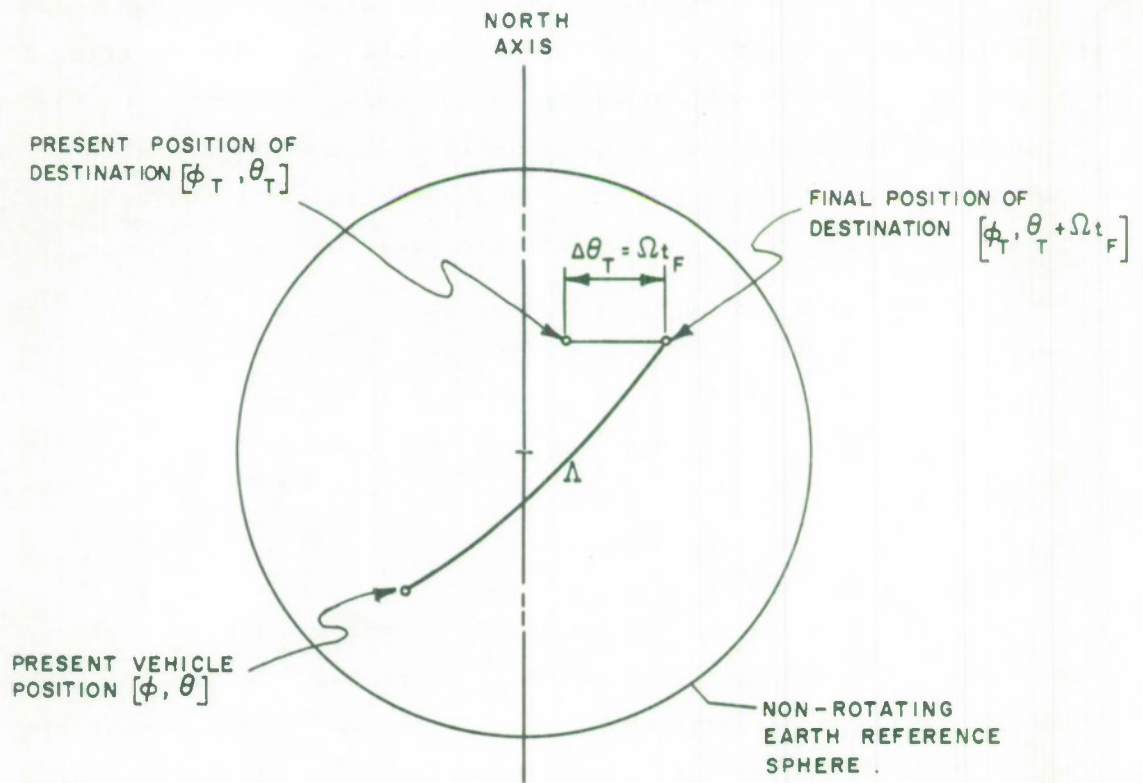
MOTION OF DESTINATION ON FIXED REFERENCE SPHERE

FIG. C-2

IA-13110

C-53

and

$$\theta_{T_F} = \theta_T + \Omega t_F \qquad (C\text{-}9)$$

The angle Ωt_F in the last equation is the angle through which the earth rotates in the remaining time of flight, t_F. The equation for estimating t_F, derived in Appendix B (Eq. B-26), contains the factor $\frac{L}{D} \cos \sigma_A$. It is shown in a later section of this appendix that the guidance system attempts to drive this quantity to the value $\frac{1}{2} \left[(\frac{L}{D})_{MAX} + (\frac{L}{D})_{MIN} \right]$. Therefore, with the latter expression used in place of the $\frac{L}{D} \cos \sigma_A$, Eq. B-26 can be approximated as

$$t_F = \frac{V_c}{4g} \left[\left(\frac{L}{D}\right)_{MAX} + \left(\frac{L}{D}\right)_{MIN} \right] \ln \left[\frac{1 + \dfrac{V_A}{V_c}}{1 - \dfrac{V_A}{V_c}} \right] \qquad (C\text{-}10)$$

NORMALIZED ERROR SIGNALS

Guidance commands are computed from error quantities representing the amount by which the destination is displaced from the GAA center. However, to match the magnitudes of the commands to the maneuvering capabilities of the vehicle at all times, the computed errors are normalized. When the destination is centered in the GAA, errors are zero, and when the destination coincides with one of the cardinal points the magnitude of the corresponding error is unity. Normalized lateral error, used in determining the required bank angle, is as follows:

$$\Delta R_c^* = \frac{\mu}{\nu} \qquad (C\text{-}11)$$

Normalized longitudinal error, used to compute required $\frac{L}{D}$, is given by the following equation:

$$\Delta R_D^* = \frac{2\lambda - \lambda_{MAX} - \lambda_{MIN}}{\lambda_{MAX} - \lambda_{MIN}} \qquad (C-12)$$

PHUGOID DAMPING

Bank angle command is based on normalized errors alone. Lift-to-drag ratio command, on the other hand, has two components: one based on ΔR_D^* and the other based on the vehicle's instantaneous altitude rate. The latter component has the function of damping out the phugoid oscillation in the trajectory.

The phugoid oscillation is a lightly-damped oscillatory deviation from a smooth, monotonic trajectory. The nature of the phenomenon is illustrated in Fig. 8 of the main body of this paper. If the flight conditions of a re-entry glider flying at constant $\frac{L}{D}$ Cos σ deviate from those for an equilibrium glide at that value of $\frac{L}{D}$ Cos σ, a phugoid oscillation is induced. The mechanism of the oscillation hinges on the variation of atmospheric density with altitude, and is discussed in some detail in Refs. 2 and 7.

If phugoid oscillations are not controlled, vehicle acceleration and skin temperatures will have an oscillatory history and may reach intolerably high peak values. It is therefore desirable to damp the oscillations by varying $\frac{L}{D}$ Cos σ, and avoid high peak accelerations and temperatures. In the present system, the required damping signal is derived from the difference between the vehicle's altitude rate and that which the vehicle would have if it were on a reference equilibrium glide trajectory with its present velocity. It is shown in Appendix B that this equilibrium altitude rate is

$$\dot{h}_e = - \frac{2g}{kV_A \left(\frac{L}{D} \right) \text{Cos } \sigma} \qquad (C-13)$$

The damping signal takes the form of an increment in the commanded value of $\frac{L}{D}$ Cos σ, proportional to the difference in altitude rates:

C-55

$$\Delta \left(\frac{L}{D} \cos \sigma \right) \alpha \left(\dot{h} - \dot{h}_e \right)$$

Reference 2 shows that a more nearly constant damping ratio can be achieved throughout the flight by making the proportionality constant in turn proportional to vehicle velocity. Thus,

$$\Delta \left(\frac{L}{D} \cos \sigma \right) = K_D V_A \left(\dot{h} - \dot{h}_e \right) \qquad (C-14)$$

GUIDANCE COMMANDS

Bank Angle

Commanded bank angle σ is made directly proportional to the normalized lateral error, with a proportionality constant weighted by the normalized longitudinal error:

$$\sigma = \left[K_{\sigma c} - K_{\sigma D} \, \Delta R_D^* \right] \Delta R_c^* \qquad (C-15)$$

This angle is not allowed to exceed certain limits, however:

$$|\sigma| \leq \sigma_{MAX}. \qquad (C-16)$$

If the angle computed from Eq. C-15 falls outside this allowable range, the value of the nearest limit is used instead. The angle determined by Eqs. C-15 and C-16 is used in the subsequent calculation of the $\frac{L}{D}$ command.

Lift-to-Drag Ratio

As Appendix B shows, longitudinal range is determined by the quantity $\frac{L}{D} \cos \sigma$. Lift-to-drag ratio command is computed by determining the required value of $\frac{L}{D} \cos \sigma$ and dividing this by $\cos \sigma$.

The first of the two components of $\frac{L}{D} \cos \sigma$ is based on ΔR_D^*. When ΔR_D^* is zero, $\frac{L}{D} \cos \sigma$ must have a value corresponding to the landing point halfway between the two longitudinal cardinal points:

$$\left[\frac{L}{D} \cos \sigma \right]_{\Delta R_D^* = 0} = \frac{1}{2} \left[\left(\frac{L}{D} \right)_{MAX.} + \left(\frac{L}{D} \right)_{MIN.} \right] \qquad (C\text{-}17)$$

Non-zero values of ΔR_D^* call for variations in $\frac{L}{D} \cos \sigma$ from this central value. The function used to relate $\frac{L}{D} \cos \sigma$ to ΔR_D^* is given in Fig. C-3. The non-linearity of this function provides an over-control feature. which tends to center the GAA over the destination more quickly than would a function linear throughout the range $-1 \le \Delta R_D^* \le +1$.

This component of $\frac{L}{D} \cos \sigma$ is called the nominal value, and can be expressed analytically as follows:

For $\Delta R_D^* \le - \Delta R_{DL}^*$:

$$\left[\frac{L}{D} \cos \sigma \right]_{NOM.} = \left[\frac{L}{D} \right]_{MIN.} \cos \sigma \qquad (C\text{-}18a)$$

For $- \Delta R_{DL}^* < \Delta R_{DL}^* \le 0$:

$$\left[\frac{L}{D} \cos \sigma \right]_{NOM.} = \frac{1}{2} \left[1 + \frac{\Delta R_D^*}{\Delta R_{DL}^*} \right] \left[\left(\frac{L}{D} \right)_{MAX.} + \left(\frac{L}{D} \right)_{MIN.} \right]$$

$$- \frac{\Delta R_D^*}{\Delta R_{DL}^*} \left[\frac{L}{D} \right]_{MIN.} \cos \sigma \qquad (C\text{-}18b)$$

For $0 < \Delta R_D^* < \Delta R_{DL}^*$:

$$\left[\frac{L}{D} \cos \sigma \right]_{NOM.} = \frac{1}{2} \left[1 - \frac{\Delta R_D^*}{\Delta R_{DL}^*} \right] \left[\left(\frac{L}{D} \right)_{MAX.} + \left(\frac{L}{D} \right)_{MIN.} \right]$$

$$+ \frac{\Delta R_D^*}{\Delta R_{DL}^*} \left[\frac{L}{D} \right]_{MAX.} \cos \sigma \qquad (C\text{-}18c)$$
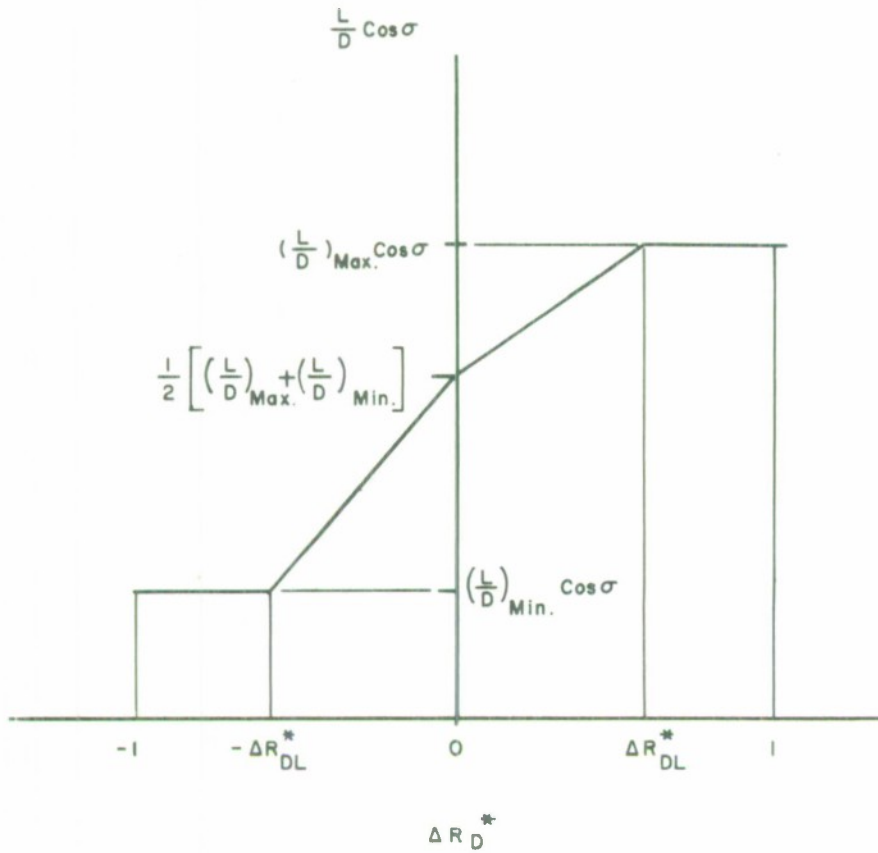
RELATIONSHIP BETWEEN COMMANDED $\frac{L}{D} \cos\sigma$
AND NORMALIZED LONGITUDINAL ERROR

FIG. C-3

For $\Delta R_D^* \geq \Delta R_{DL}^*$:

$$\left[\frac{L}{D} \cos \sigma\right]_{NOM.} = \left[\frac{L}{D}\right]_{MAX.} \cos \sigma \qquad \text{(C-18d)}$$

The second component of the $\frac{L}{D} \cos \sigma$ command is the phugoid damping term, Eq. C-14. The equilibrium altitude rate $\dot{h}_e$ used in computing this quantity is based on the nominal value of $\frac{L}{D} \cos \sigma$ immediately above. When the damping term is expanded by the use of Eq. C-13 and added to the nominal value, the final $\frac{L}{D} \cos \sigma$ command is produced:

$$\frac{L}{D} \cos \sigma = \left[\frac{L}{D} \cos \sigma\right]_{NOM.} + K_D V_A \left[\dot{h} + \frac{2g}{kV_A\left[\frac{L}{D} \cos \sigma\right]_{NOM.}}\right] \qquad \text{(C-19)}$$

Lift-to-drag ratio is developed by simply dividing the last equation by $\cos \sigma$.

Finally, the command generated in this way is subjected to a limiting process, to keep the lift-to-drag ratio of the vehicle within specified limits at all times:

$$\left[\frac{L}{D}\right]_{MIN.} \leq \frac{L}{D} \leq \frac{L}{D}_{MAX.} \qquad \text{(C-20)}$$

If the value of $\frac{L}{D}$ computed from Eq. C-19 falls outside the allowable range (Eq. C-20), the nearest limiting value is used instead.

a	=	Downrange central angle.
A	=	Reference area.
A_i	=	Azimuth angle from tracking station i to vehicle.
b	=	Crossrange central angle.
c	=	Central angle between initial and present positions.
C_D	=	Drag coefficient.
C_L	=	Lift coefficient.
D	=	Aerodynamic drag force.
E_i	=	Elevation angle of line of sight from tracking station i to vehicle.
F	=	Resultant force on vehicle.
F_N	=	Vehicle stagnation point design parameter (ft.)
g	=	Local gravitational acceleration.
g_e	=	Gravitational acceleration at earth's surface.
G	=	Universal gravitational constant
h	=	Vehicle altitude (positive upward).
h_i	=	Elevation of tracking station i above reference spherical earth.
k	=	Exponential decay parameter of earth's atmospheric density.
K_D	=	Phugoid damping gain constant $(\sec.^2/ft.^2)$.
K_{WB}	=	Wing bottom temperature constant $\dfrac{(^oR)(\sec)^{0.467}}{(lb.)^{0.2}(ft.)^{0.067}}$
$K_{\sigma c}$	=	Bank angle gain constant (degrees).
$K_{\sigma D}$	=	Bank angle cross-coupling gain constant (degrees).
L	=	Lift force.
m	=	Mass of vehicle.
M	=	Mass of the earth
n	=	Resultant specific force per unit mass on the vehicle (in units of earth's-surface g's).
n_L	=	Longitudinal component of specific force per unit mass (in earth's-surface g's).

n_N	=	Lateral component of specific force per unit mass (in earth's-surface g's).
q	=	Dynamic pressure
r	=	Vehicle's radius from earth's center
r_i	=	Radius from earth's center to tracking station i.
R_e	=	Radius of the earth.
R_i	=	Line-of-sight range between vehicle and tracking station i
R_N	=	Radius of vehicle structure at stagnation point (ft.)
ΔR_c^*	=	Normalized lateral guidance error
ΔR_D^*	=	Normalized longitudinal guidance error
ΔR_{DL}^*	=	Lift-to-drag ratio gain parameter.
S	=	Horizontal distance traveled by vehicle.
t	=	Time
t_F	=	Length of flight time remaining at any instant.
T_s	=	Stagnation-point skin temperature (^{O}F. abs.)
T_{WB}	=	Wing-bottom temperature. (^{O}F. abs.).
V	=	Vehicle velocity with respect to the rotating earth.
V_A	=	Vehicle velocity with respect to an inertial reference frame.
V_c	=	Inertial velocity of a satellite in circular orbit at the vehicle's present altitude above the earth ($= gr$).
x_i, y_i, z_i	=	Vehicle position components with respect to coordinate system centered at tracking station i.
α	=	Angle of attack (positive upward)
β	=	Angle between vehicle's local meridian and great circle between sub-vehicle point and destination (Fig. C-1). [Symbol β also used for longitude with respect to vernal equinox line (Fig. 1)]
γ	=	Flight path angle (positive above horizontal)

ϵ_N = Emissivity of vehicle skin at stagnation point.

η = Heading with respect to north (positive clockwise).

θ = Vehicle longitude (positive easterly)

θ_i = Longitude of tracking station i (positive easterly).

θ_T = Longitude of destination (positive easterly).

λ = Earth central angle covered by re-entry vehicle at zero bank angle.

Λ = Great circle arc from sub-vehicle point to destination. (Fig. C-1).

μ = Great circle arc from destination to reference great circle. (Fig. C-1).

ν = Great circle arc from lateral cardinal point of GAA to reference great circle. (Fig. C-1).

ξ = Angle between vehicle's local meridian and reference great circle. (Fig. C-1).

ρ = Local air density.

ρ_{SL} = Atmospheric density at surface of the earth.

σ = Bank angle (positive for right wing down).

φ = Vehicle latitude (positive northerly)

φ_i = Latitude of tracking station i (positive northerly).

φ_T = Latitude of destination (positive northerly)

ψ = Angle between vehicle's initial local meridian and great circle between initial sub-vehicle point and present sub-vehicle point.

ω = Angular velocity of rotating coordinate system.

Ω = Earth's angular velocity.

D-63

APPENDIX E

REFERENCES

1. Wingrove, R. C., "Survey of Atmosphere Re-entry Guidance and Control Methods", AIAA Journal 1, 2019-2029 (September 1963).

2. "Study and Preliminary Design of an Energy Management Computer for Winged Vehicles", USAF Aeronautical Systems Division, Technical Documentary Report No. ASD-TDR-62-51 (March 1962).

3. Dow, P. C., Jr., Fields, D. P., and Scammell, F. H., "Automatic Re-Entry Guidance at Escape Velocity", ARS Preprint No. 1946-61 (August 1961).

4. Terasaki, R. M., "A Guidance Scheme for Lifting Re-Entry", AIAA Preprint No. 63-320 (August 1963).

5. Duncan, R. C., Dynamics of Atmospheric Entry, McGraw-Hill Book Company, New York, 1962.

6. Goldstein, H., Classical Mechanics, Addison-Wesley Publishing Company, Reading, Massachusetts, 1959.

7. Schofield, B. L., and Hoey, R. G., "Cockpit Displays for Optimizing Pilot Control During Re-entry", Proceedings of the 1962 X-20A (Dyna-Soar) Symposium, Vol. II, Flight Mechanics and Guidance, USAF Aeronautical Systems Division, Technical Documentary Report No. ASD-TDR-63-148, Vol. II (March 1963).

DOCUMENT CONTROL DATA - R&D

(Security classification of title, body of abstract and indexing annotation must be entered when the overall report is classified)

1. ORIGINATING ACTIVITY *(Corporate author)*	2a. REPORT SECURITY CLASSIFICATION
MITRE CORPORATION BEDFORD, MASSACHUSETTS	UNCLASSIFIED
	2b. GROUP N/A

3. REPORT TITLE

A RE-ENTRY VEHICLE SIMULATION DESIGNED FOR THE STUDY OF GROUND SYSTEM RE-QUIREMENTS

4. DESCRIPTIVE NOTES *(Type of report and inclusive dates)*

5. AUTHOR(S) *(Last name, first name, initial)*

PLENDER, P.J.

6. REPORT DATE JULY XX 64	7a. TOTAL NO. OF PAGES 82	7b. NO. OF REFS 7
8a. CONTRACT OR GRANT NO. AF19(628)2390	9a. ORIGINATOR'S REPORT NUMBER(S)	
b. PROJECT NO. c. 611.1	TM-03973	
d.	9b. OTHER REPORT NO(S) *(Any other numbers that may be assigned this report)* ESD-TDR-64-135	

10. AVAILABILITY/LIMITATION NOTICES

QUALIFIED REQUESTERS MAY OBTAIN COPIES FROM DDC.
AVAL FROM OTS.

11. SUPPLEMENTARY NOTES NONE	12. SPONSORING MILITARY ACTIVITY Deputy For Advanced Planning ESD, L.G. HANSCOM FIELD, BEDFORD, MASS.

13. ABSTRACT

A computer simulation of re-entry vehicle trajectories has been developed as an aid in determining the requirements of supporting ground-based electronic system. This report describes the mathematical model used in this simulation and discusses, with the aid of examples, the usefulness of the output data in the preliminary design of tracking and communications networks.

DD FORM 1 JAN 64 1473

14. KEY WORDS	LINK A		LINK B		LINK C	
	ROLE	WT	ROLE	WT	ROLE	WT
COMPUTER						
RE-ENTRY						
TRAJECTORIES						
TRACKING						
COMMUNICATIONS						
BALLISTICS						
SPACE						
MISSILE						
ELECTRONIC SYSTEMS						
ANALOG						
DIGITAL						

INSTRUCTIONS

1. ORIGINATING ACTIVITY: Enter the name and address of the contractor, subcontractor, grantee, Department of Defense activity or other organization (corporate author) issuing the report.

2a. REPORT SECURITY CLASSIFICATION: Enter the overall security classification of the report. Indicate whether "Restricted Data" is included. Marking is to be in accordance with appropriate security regulations.

2b. GROUP: Automatic downgrading is specified in DoD Directive 5200.10 and Armed Forces Industrial Manual. Enter the group number. Also, when applicable, show that optional markings have been used for Group 3 and Group 4 as authorized.

3. REPORT TITLE: Enter the complete report title in all capital letters. Titles in all cases should be unclassified. If a meaningful title cannot be selected without classification, show title classification in all capitals in parenthesis immediately following the title.

4. DESCRIPTIVE NOTES: If appropriate, enter the type of report, e.g., interim, progress, summary, annual, or final. Give the inclusive dates when a specific reporting period is covered.

5. AUTHOR(S): Enter the name(s) of author(s) as shown on or in the report. Enter last name, first name, middle initial. If military, show rank and branch of service. The name of the principal author is an absolute minimum requirement.

6. REPORT DATE: Enter the date of the report as day, month, year; or month, year. If more than one date appears on the report, use date of publication.

7a. TOTAL NUMBER OF PAGES: The total page count should follow normal pagination procedures, i.e., enter the number of pages containing information.

7b. NUMBER OF REFERENCES: Enter the total number of references cited in the report.

8a. CONTRACT OR GRANT NUMBER: If appropriate, enter the applicable number of the contract or grant under which the report was written.

8b, 8c, & 8d. PROJECT NUMBER: Enter the appropriate military department identification, such as project number, subproject number, system numbers, task number, etc.

9a. ORIGINATOR'S REPORT NUMBER(S): Enter the official report number by which the document will be identified and controlled by the originating activity. This number must be unique to this report.

9b. OTHER REPORT NUMBER(S): If the report has been assigned any other report numbers (either by the originator or by the sponsor), also enter this number(s).

10. AVAILABILITY/LIMITATION NOTICES: Enter any limitations on further dissemination of the report, other than those imposed by security classification, using standard statements such as:

(1) "Qualified requesters may obtain copies of this report from DDC."

(2) "Foreign announcement and dissemination of this report by DDC is not authorized."

(3) "U. S. Government agencies may obtain copies of this report directly from DDC. Other qualified DDC users shall request through

_____ ."

(4) "U. S. military agencies may obtain copies of this report directly from DDC. Other qualified users shall request through

_____ ."

(5) "All distribution of this report is controlled. Qualified DDC users shall request through

_____ ."

If the report has been furnished to the Office of Technical Services, Department of Commerce, for sale to the public, indicate this fact and enter the price, if known.

11. SUPPLEMENTARY NOTES: Use for additional explanatory notes.

12. SPONSORING MILITARY ACTIVITY: Enter the name of the departmental project office or laboratory sponsoring (paying for) the research and development. Include address.

13. ABSTRACT: Enter an abstract giving a brief and factual summary of the document indicative of the report, even though it may also appear elsewhere in the body of the technical report. If additional space is required, a continuation sheet shall be attached.

It is highly desirable that the abstract of classified reports be unclassified. Each paragraph of the abstract shall end with an indication of the military security classification of the information in the paragraph, represented as (TS), (S), (C), or (U).

There is no limitation on the length of the abstract. However, the suggested length is from 150 to 225 words.

14. KEY WORDS: Key words are technically meaningful terms or short phrases that characterize a report and may be used as index entries for cataloging the report. Key words must be selected so that no security classification is required. Identifiers, such as equipment model designation, trade name, military project code name, geographic location, may be used as key words but will be followed by an indication of technical context. The assignment of links, rules, and weights is optional.